

Supporting information

**Generation, regeneration, and recovery of Cu catalytic system by
changing the polarity of electrodes**

Konstantin S. Rodygin,^a Dmitriy E. Samoylenko,^a Marina M. Seitkalieva,^b Kristina A. Lotsman,^a
Svetlana A. Metlyaeva,^a and Valentine P. Ananikov*^{a,b}

^aSaint Petersburg State University, Universitetskiy pr. 26, Stary Petergof 198504, Russia.

^bN. D. Zelinsky Institute of Organic Chemistry, Russian Academy of Sciences, Leninsky pr. 47,
Moscow 119991, Russia. E-mail: val@ioc.ac.ru.

Contents

S1. CV MEASUREMENTS	3
S2. OPTIMIZATION EXPERIMENTS	7
S3. NMR DATA AND CHARACTERIZATION	10
S4. NMR SPECTRA	13
S5. XRD DATA	29
S6. SEM DATA	30
S7. HRESI-MS DATA.....	32
S8. SINGLE CRYSTAL X-RAY STRUCTURE DETERMINATION	33
S9. DETAILS ON ELECTROCHEMICAL EXPERIMENTS	35
S10. REFERENCES	39

S1. CV measurements

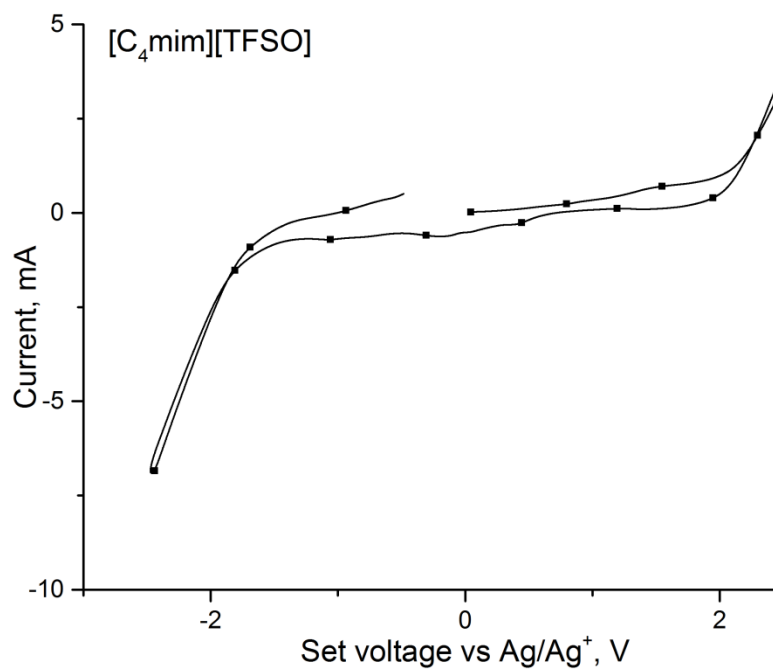


Figure S1. Cyclic voltammogram of [C₄mim][TFSO].

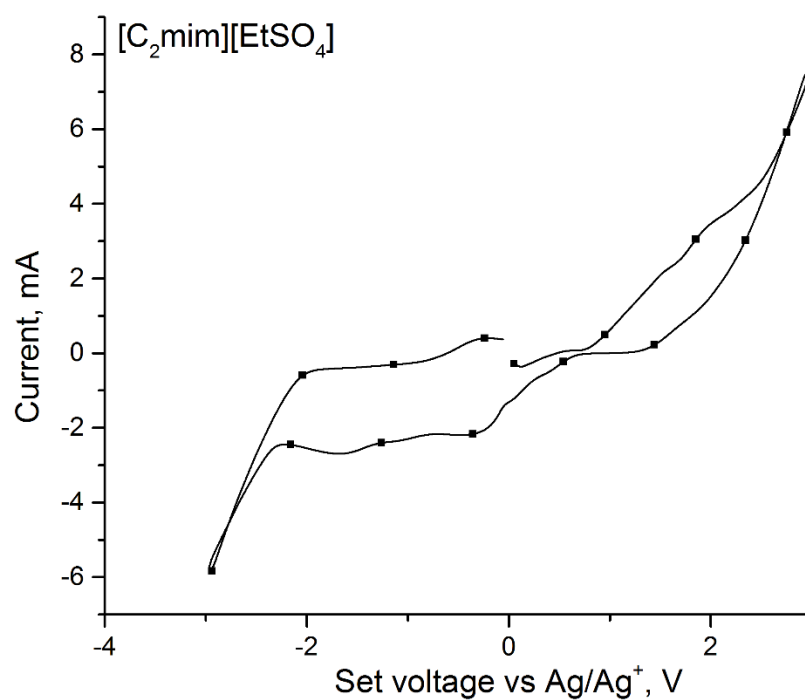


Figure S2. Cyclic voltammogram of [C₂mim][EtSO₄]

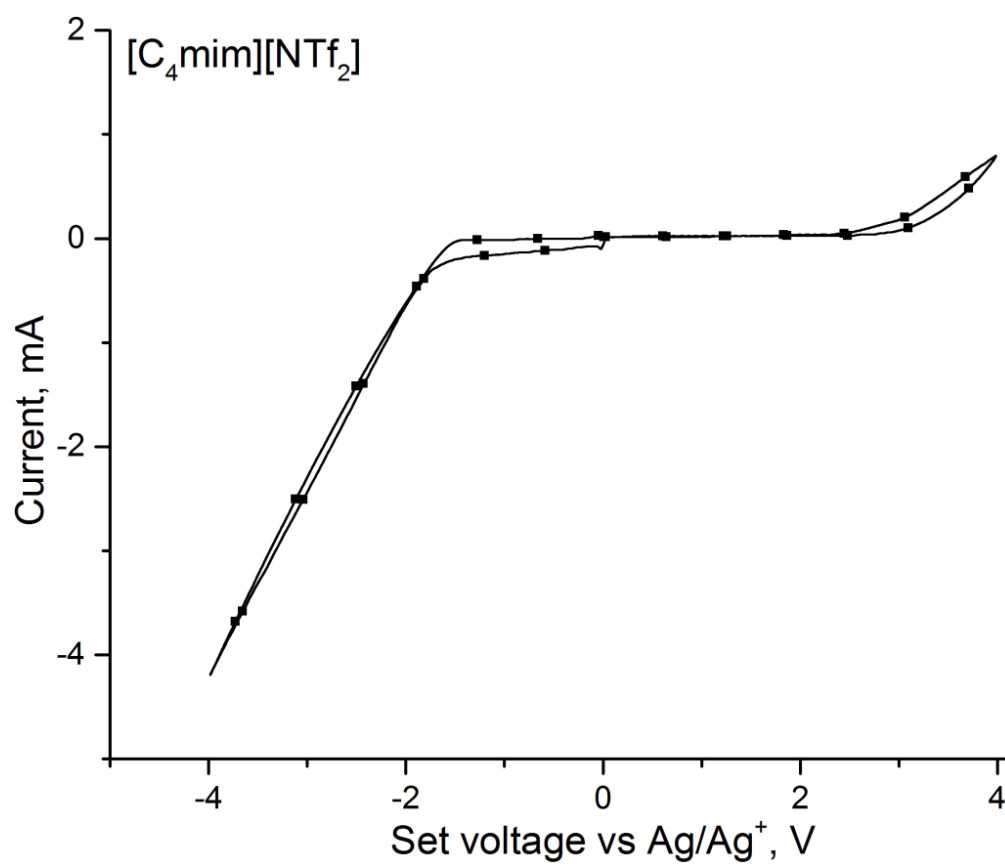


Figure S3. Cyclic voltammogram of [C₄mim][NTf₂]

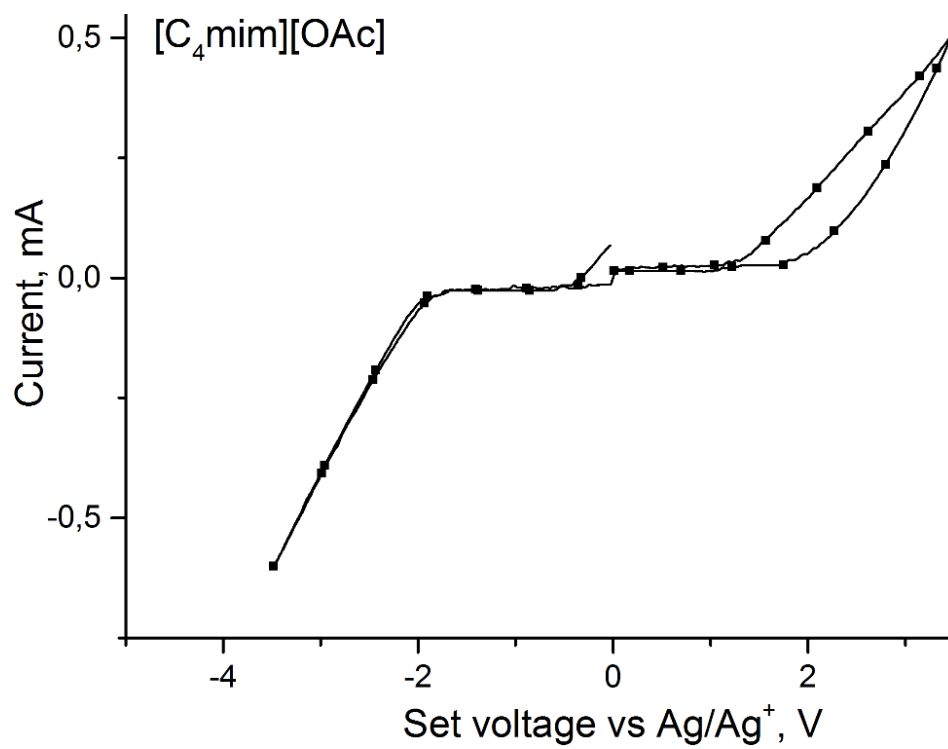


Figure S4. Cyclic voltammogram of [C₄mim][OAc]

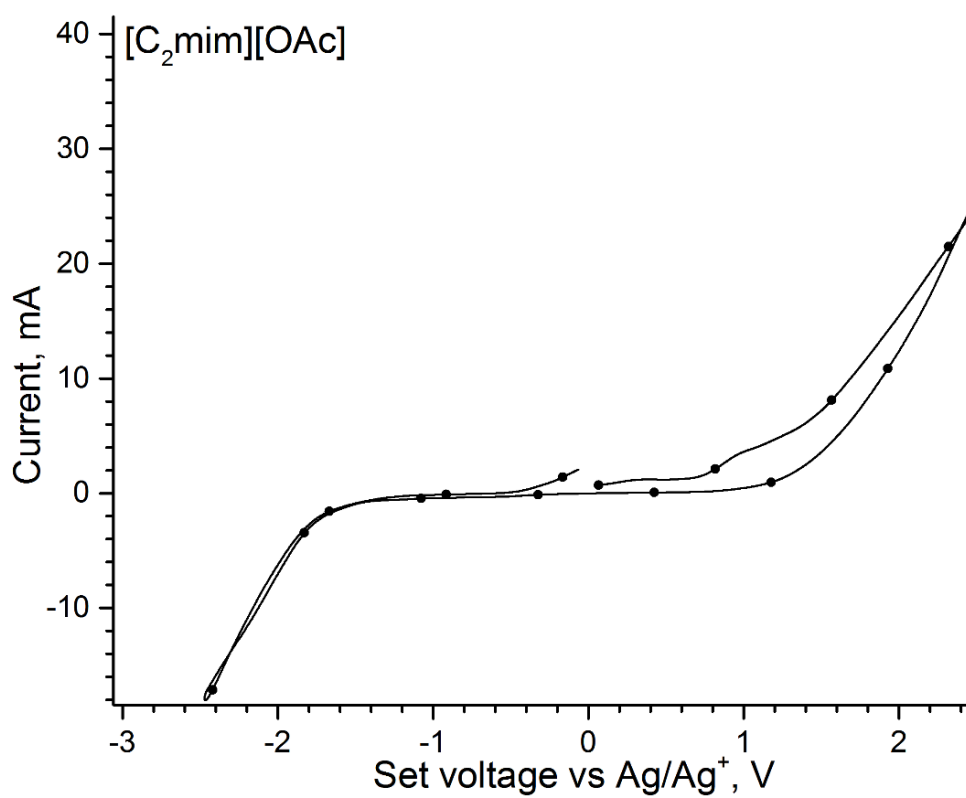


Figure S5. Cyclic voltammogram of [C₂mim][OAc]

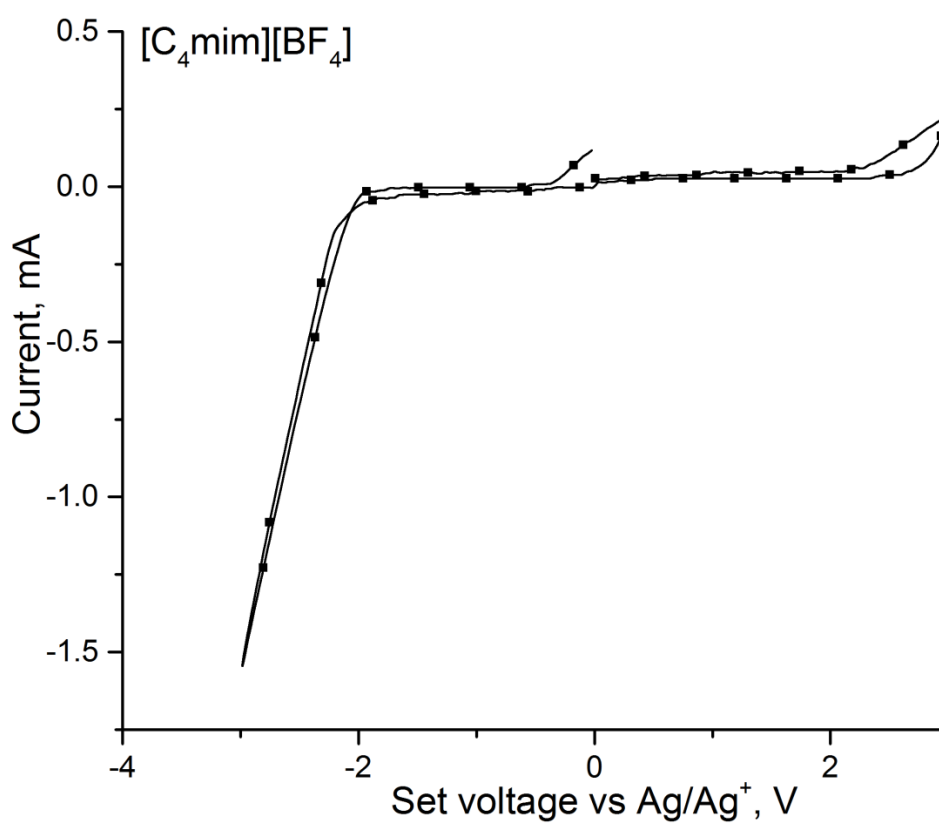


Figure S6. Cyclic voltammogram of [C₄mim][BF₄]

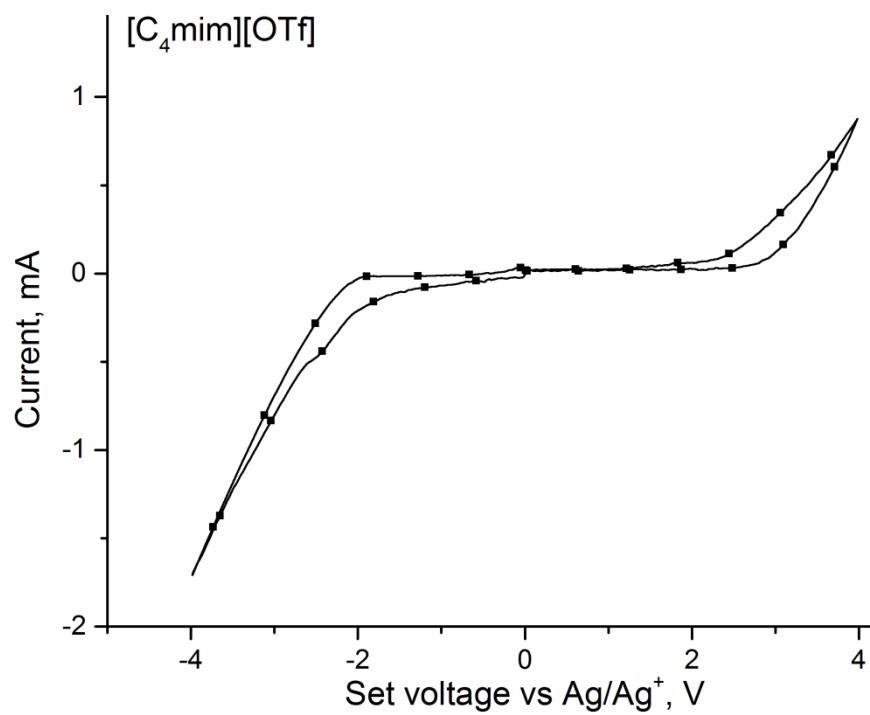


Figure S7. Cyclic voltammogram of [C₄mim][OTf]

S2. Optimization experiments

Optimization of copper electrode dissolution in different ILs.

Table S1. Optimization of electrochemical dissolution of a copper electrode in ILs with C₂mim⁺ cation.

№	IL	V(H ₂ O), vol%	t, h	I, mA	m(Cu), mg
1	[C ₂ mim][EtSO ₄]	0	1.5	2	4.6
2	[C ₂ mim][OAc]	0	1.5	2	1.2
3	[C ₄ mim][HSO ₄]	0	1.5	2	0
4	[C ₂ mim][EtSO ₄]	0	1.5	0.2	0.7
5	[C ₂ mim][OAc]	5	1	2	4.1
6	[C ₂ mim][OAc]	5	1.5	2	5.8
7	[C ₂ mim][OAc]	10	0.5	2	0.7
8	[C ₂ mim][OAc]	10	1	2	4.1
9	[C ₂ mim][OAc]	10	1.5	2	7.7

At the first stage, ILs were selected ([C₂mim][EtSO₄], [C₂mim][OAc], [C₄mim][HSO₄]), in which the electrochemical dissolution of the copper electrode was carried out without the addition of water (Table S1, ent. 1–3). It was noted that the process proceeds better in IL based on 1-ethyl-3-methylimidazolium than in [C₄mim][HSO₄]. Since [C₂mim][EtSO₄] showed the best efficiency in dissolving copper, we tried to use this IL to change the direct current to 0.2 mA (Table S1, ent. 4). This led to a significant decrease in the amount of dissolved copper in the solution, so it was decided to conduct experiments with a current of 2 mA. Since [C₂mim][EtSO₄], [C₂mim][OAc] also showed promising results in the dissolution of the copper electrode, we decided to use this IL to test the possibility of increasing the efficiency of copper dissolution by adding water into the system. As expected, already with the addition of 5 vol.% of water for 1 h, the efficiency of dissolving copper by electric current is comparable to that obtained with [C₂mim][EtSO₄] (Table S1, ent. 5). The higher the dissolution time, the much copper transferred to the solution (Table S1, entry 6). The addition of 10 vol.% also increases the efficiency of copper dissolution, and by varying the time, we were able to achieve the dissolution of 7.7 mg of copper in IL (Table S1, ent. 7-9).

Table S2. Optimization of anodic dissolution of a copper electrode in ILs with C₄mim⁺ cation*.

№	IL	V(H ₂ O), %	Ua, V	m(Cu), g
1	[C ₄ mim][BF ₄]	0	2.4 – 2.5	0.0003
2	[C ₄ mim][BF ₄]	5	2.4	0.0009
3	[C ₄ mim][OTf]	0	2.1	0.0015
4	[C ₄ mim][OTf]	5	2.1	0.0016
5	[C ₄ mim][OAc]	0	1.4	0.0019
6	[C ₄ mim][OAc]	5	1.36	0.0011
7	[C ₄ mim][NTf ₂]	0	2.4	0.0008
8	[C ₄ mim][NTf ₂]	5	2.4	0.0006

* Dissolution time is 2 h; current is 0.3 mA.

Without water the mass of dissolved copper varied from 0.3 mg ([C₄mim][BF₄]) to 1.9 mg ([C₄mim][OAc]) (Table 1). When the 5 vol.% of water was added the mass of dissolved copper was changed. In case of [C₄mim][BF₄] the mass increases to 0.9 mg, whereas in other cases it did not change significantly ([C₄mim][TfO] and [C₄mim][NTf₂]) or decreased to 1.1 mg ([C₄mim][OAc]), compared to the conditions without added water. To obtain Cu-contained IL solution for C-S cross-coupling reactions the current was increased to 2 mA, which lead to an increase in the mass of released copper, similar to experiments in ILs with C₂mim-cation.

Table S3. Optimization of ILs for C–S cross coupling reaction*

№	IL	V(H ₂ O), vol.%	Conversion (%)
1.	[C ₄ mim][BF ₄]	0	38
2.		5	29
3.	[C ₄ mim][OTf]	0	41
4.		5	15
5.	[C ₄ mim][OAc]	0	<1
6.		5	7
7.	[C ₄ mim][NTf ₂]	0	12
8.		5	12

*2 h, 110 °C

In 2 h the best results were achieved in [C₄mim][BF₄] and [C₄mim][OTf] ILs. In the case of [C₂mim][OTF] the product was not isolated due to good miscibility of the IL with common organic solvents for the extraction. Therefore, the reaction was carried out in [C₄mim][BF₄] IL with different amount of water for 24 h.

Table S4. Copper-catalyzed C–S cross coupling reaction optimization in [C₄mim][BF₄] IL.

№	H ₂ O, vol.%	t, h	Conversion, %
1	0	24	80
2	1	24	85
3	5	24	93
4	10	24	90

1.2 eq. Cs₂CO₃, 5 mol.% Cu, 110 °C

The best results were obtained in a system with 5 vol.% of water.

Calcium carbide in copper-promoted “click”-reaction.

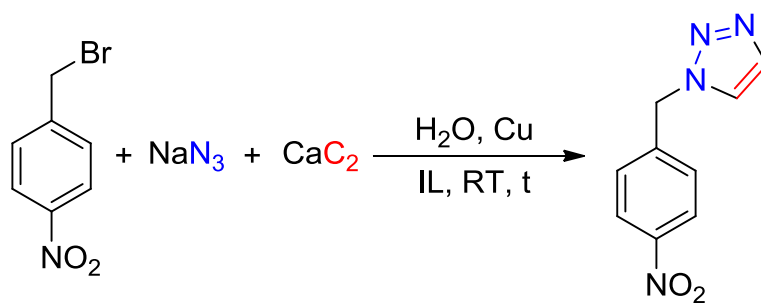


Table S5. Optimization of carbide-based synthesis of triazoles (**16-17**).

No	IL	t, h	C-electrode	H ₂ O, mL	Δm (Cu-electrode), mg	NMR yield, %
1	[C ₂ mim][HSO ₄]	2	Stainless steel	0.2	-	NR
2	[C ₄ mim][PF ₆]	2	Stainless steel	0.2	5.2	NR
3	[C ₂ mim][OAc]	2	Stainless steel	0.2	4.9	NR
4	[C ₄ mim][BF ₄]	2	Stainless steel	0.2	2.8	63
5	[C ₄ mpyr][BF ₄]	2	Stainless steel	0.2	6.1	72
6	[C ₂ mim][EtSO ₄]	2	Stainless steel	0.2	1.4	93
7	[C ₂ mim][EtSO ₄]	3	Graphite	0.2	6.8	99
8	[C ₂ mim][EtSO ₄]	3	Pt	0.2	5.0	99
9	[C ₂ mim][EtSO ₄]	3	Stainless steel	0.2	6.7	99
10	[C ₂ mim][EtSO ₄]	3	Stainless steel	0.1	6.6	99
11	[C ₂ mim][EtSO ₄]	3	Stainless steel	0.03	7.2	76

S3. NMR data and characterization

1,4-diphenyl-1H-1,2,3-triazole (1)

¹H NMR (400 MHz, DMSO-*d*₆) δ 9.30 (s, 1H), 7.96 (m, 4H), 7.64 (t, *J* = 7.9 Hz, 2H), 7.58 – 7.44 (m, 3H), 7.44 – 7.32 (m, 1H). ¹³C NMR (101 MHz, DMSO-*d*₆) δ 147.3, 136.6, 130.2, 129.9, 129.0, 128.7, 128.2, 125.3, 120.0, 119.6.

4-phenyl-1-(p-tolyl)-1H-1,2,3-triazole (2)

¹H NMR (400 MHz, DMSO-*d*₆) δ 9.24 (s, 1H), 8.00 – 7.88 (m, 2H), 7.83 (d, *J* = 8.3 Hz, 2H), 7.50 (t, *J* = 7.57 Hz, 2H), 7.43 (d, *J* = 8.12, 2H), 7.38 (t, *J* = 7.38, 1H), 2.39 (s, 3H). ¹³C NMR (101 MHz, DMSO-*d*₆) δ 147.2, 138.3, 134.4, 130.3, 130.2, 129.0, 128.1, 125.3, 119.8, 119.4, 20.6.

4-phenyl-1-(m-tolyl)-1H-1,2,3-triazole (3)

¹H NMR (400 MHz, DMSO-*d*₆) δ 9.27 (s, 1H), 8.01 – 7.87 (m, 2H), 7.80 (s, 1H), 7.75 (d, *J* = 8.0 Hz, 1H), 7.50 (m, 3H), 7.38 (t, *J* = 7.4 Hz, 1H), 7.33 (d, *J* = 7.6 Hz, 1H), 2.44 (s, 3H). ¹³C NMR (101 MHz, DMSO-*d*₆) δ 147.2, 139.6, 136.6, 130.3, 129.7, 129.3, 129.0, 128.2, 125.3, 120.4, 119.5, 117.1, 20.9.

4-phenyl-1-(4-chlorophenyl)-1H-1,2,3-triazole (4)

¹H NMR (400 MHz, DMSO-*d*₆) δ 9.34 (s, 1H), 8.01 (d, *J* = 8.8 Hz, 2H), 7.98 – 7.90 (m, 2H), 7.72 (d, *J* = 8.85 Hz, 2H), 7.52 (t, *J* = 7.7 Hz, 2H), 7.44 – 7.37 (m, 1H). ¹³C NMR (101 MHz, DMSO-*d*₆) δ 147.4, 135.4, 133.0, 130.1, 129.9, 129.0, 128.3, 125.3, 121.7, 119.7.

4-phenyl-1-(3,4-dichlorophenyl)-1H-1,2,3-triazole (5)

¹H NMR (400 MHz, DMSO-*d*₆) δ 9.40 (s, 1H), 8.31 (d, *J* = 2.5 Hz, 1H), 8.02 (dd, *J* = 8.7, 2.6 Hz, 1H), 7.93 (d, *J* = 7.5 Hz, 3H), 7.52 (t, *J* = 7.6 Hz, 2H), 7.40 (t, *J* = 7.4 Hz, 1H). ¹³C NMR (101 MHz, DMSO) δ 147.5, 132.4, 131.9, 131.0, 129.9, 129.0, 128.4, 125.3, 121.6, 120.0, 119.9.

4-phenyl-1-(4-fluorophenyl)-1H-1,2,3-triazole (6)

¹H NMR (400 MHz, DMSO-*d*₆) δ 9.27 (s, 1H), 8.04 – 7.97 (m, 2H), 7.97 – 7.91 (m, 2H), 7.54 – 7.46 (m, 4H), 7.44 – 7.35 (m, 1H). ¹³C NMR (101 MHz, DMSO-*d*₆) δ 161.6 (d, *J* = 245.8 Hz), 147.3, 133.2 (d, *J* = 3.0 Hz), 130.2, 129.0, 128.2, 125.3, 122.3 (d, *J* = 8.8 Hz, 2C), 119.9, 116.8 (d, *J* = 23.3 Hz, 2C).

4-phenyl-1-(2,4,6-trimethylphenyl)-1H-1,2,3-triazole (7)

¹H NMR (400 MHz, CDCl₃) δ 7.98 – 7.88 (m, 2H), 7.83 (s, 1H), 7.52 – 7.42 (m, 2H), 7.42 – 7.32 (m, 1H), 7.01 (s, 2H), 2.37 (s, 3H), 2.02 (s, 6H). ¹³C NMR (101 MHz, CDCl₃) δ 147.7, 140.2, 135.3, 133.7, 130.7, 129.3, 129.1, 128.4, 125.9, 121.6, 21.3, 17.5.

4-phenyl-1-(3-methoxyphenyl)-1H-1,2,3-triazole (8)

¹H NMR (400 MHz, DMSO-*d*₆) δ 9.31 (s, 1H), 8.04 – 7.87 (m, 2H), 7.60 – 7.45 (m, 5H), 7.43 – 7.34 (m, 1H), 7.08 (dt, *J* = 6.8, 2.3 Hz, 1H), 3.88 (s, 3H). ¹³C NMR (101 MHz, DMSO-*d*₆) δ 160.2, 147.2, 137.6, 130.8, 130.2, 128.9, 128.2, 125.3, 119.6, 114.3, 111.9, 105.6, 55.6.

4-n-hexyl-1-(p-tolyl)-1H-1,2,3-triazole (9)

¹H NMR (400 MHz, DMSO-*d*₆) δ 8.49 (s, 1H), 7.74 (d, *J* = 8.5 Hz, 2H), 7.36 (d, *J* = 8.1 Hz, 2H), 2.67 (t, *J* = 7.6 Hz, 2H), 2.36 (s, 3H), 1.65 (quint, *J* = 7.4 Hz, 2H), 1.41 – 1.19 (m, 6H), 0.85 (t, *J* = 6.9 Hz, 3H). ¹³C NMR (101 MHz, DMSO-*d*₆) δ 148.0, 137.7, 134.6, 130.1, 119.8, 119.6, 31.0, 28.8, 28.3, 25.0, 22.0, 20.5, 13.9.

4-n-pentyl-1-(4-chlorophenyl)-1H-1,2,3-triazole (10)

¹H NMR (400 MHz, DMSO-*d*₆) δ 8.59 (s, 1H), 7.92 (d, *J* = 8.8 Hz, 2H), 7.64 (d, *J* = 8.9 Hz, 2H), 2.69 (t, *J* = 7.6 Hz, 2H), 1.66 (quint, *J* = 7.3 Hz, 2H), 1.32 (m, 4H), 0.88 (t, *J* = 7.1 Hz, 3H). ¹³C NMR (101 MHz, DMSO-*d*₆) δ 148.3, 135.6, 132.5, 129.7, 121.3, 120.1, 30.8, 28.4, 24.9, 21.8, 13.8. HRMS (*m/z*): [M-H]⁺ calcd. for C₁₃H₁₇N₃Cl, 250.1106; found, 250.1106

1-(4-nitrophenyl)-1H-1,2,3-triazole (11)

Since the reaction ended with the formation of undividable mixture, the spectrum was not defined.

4-phenyl-1-(4-nitrobenzyl)-1H-1,2,3-triazole (12)

¹H NMR (400 MHz, DMSO-*d*₆) δ 8.69 (s, 1H), 8.25 (d, *J* = 8.8 Hz, 2H), 7.90 – 7.81 (m, 2H), 7.58 (d, *J* = 8.8 Hz, 2H), 7.44 (t, *J* = 7.7 Hz, 2H), 7.33 (t, *J* = 7.4 Hz, 1H), 5.85 (s, 2H). ¹³C NMR (101 MHz, DMSO-*d*₆) δ 147.2, 146.8, 143.3, 130.5, 128.9, 128.9, 127.9, 125.2, 123.9, 121.9, 52.1.

2-(1-(4-nitrobenzyl)-1H-1,2,3-triazol-4-yl)propan-2-ol (13)

¹H NMR (400 MHz, CDCl₃) δ 8.22 (d, *J* = 8.7 Hz, 2H), 7.44 (s, 1H), 7.41 (d, *J* = 8.7 Hz, 1H), 5.61 (s, 2H), 2.56 (s, 1H), 1.62 (s, 6H). ¹³C NMR (101 MHz, CDCl₃) δ 156.7, 148.2, 141.8, 128.8, 124.4, 119.5, 68.7, 53.2, 30.6 HRMS (*m/z*): [M-H]⁺ calcd., 263.1139; found, 263.1137.

1-(4-nitrobenzyl)-4-hexyl-1H-1,2,3-triazole (14)

¹H NMR (400 MHz, CDCl₃) δ 8.22 (d, *J* = 8.1 Hz, 2H), 7.38 (d, *J* = 8.5 Hz, 2H), 7.25 (s, 1H), 5.61 (s, 2H), 2.71 (t, *J* = 7.7 Hz, 2H), 1.69 – 1.61 (m, 2H), 1.37 – 1.20 (m, 6H), 0.85 (t, *J* = 6.52 Hz, 3H).

1-(4-nitrobenzyl)-4-pentyl-1H-1,2,3-triazole (15)

¹H NMR (400 MHz, CDCl₃) δ 8.20 (d, *J* = 8.7 Hz, 2H), 7.39 (s, *J* = 8.6 Hz, 2H), 7.26 (s, 1H), 5.60 (s, 2H), 2.70 (t, *J* = 7.74 Hz, 2H), 1.65 (quint, *J* = 7.4 Hz, 2H), 1.37 – 1.28 (m, 4H), 0.87 (t, *J* = 6.14 Hz, 3H).

1-(4-nitrobenzyl)-1H-1,2,3-triazole (16)

¹H NMR (400 MHz, CDCl₃) δ 8.21 (d, *J* = 8.7 Hz, 2H), 7.76 (s, 1H), 7.58 (s, 1H), 7.39 (d, *J* = 8.7 Hz, 2H), 5.69 (s, 2H). ¹³C NMR (101 MHz, CDCl₃) δ 148.2, 141.9, 134.8, 128.6, 124.4, 123.8, 53.0.

1-benzyl-1H-1,2,3-triazole (17)

¹H NMR (400 MHz, CDCl₃) δ 7.67 (s, 1H), 7.47 (s, 1H), 7.41 – 7.27 (m, 3H), 7.27 – 7.19 (m, 2H), 5.53 (s, 2H). ¹³C NMR (101 MHz, CDCl₃) δ 134.8, 134.3, 129.1, 128.8, 128.0, 123.4, 54.0.

4-methoxyphenyl phenyl sulfide (yellow oil) (18)

¹H NMR (300 MHz, DMSO-*d*₆) δ 7.41 (2H, m), 7.30 (2H, m), 7.10 – 7.22 (3H, m), 7.01 (2H, m), 3.78 (3H, s).

S4. NMR spectra

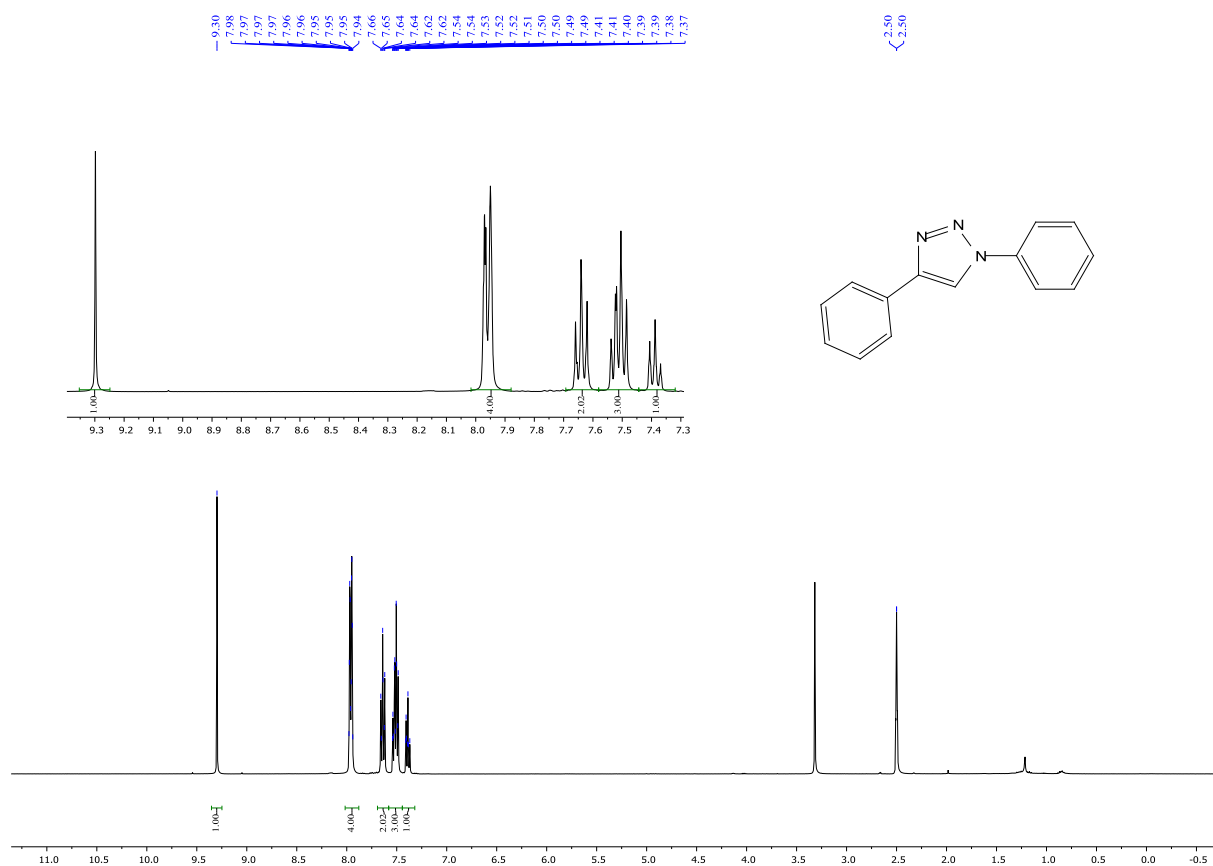


Figure S8. ¹H NMR (400 MHz, DMSO-*d*₆) spectrum of 1,4-diphenyl-1*H*-1,2,3-triazole (**1**)

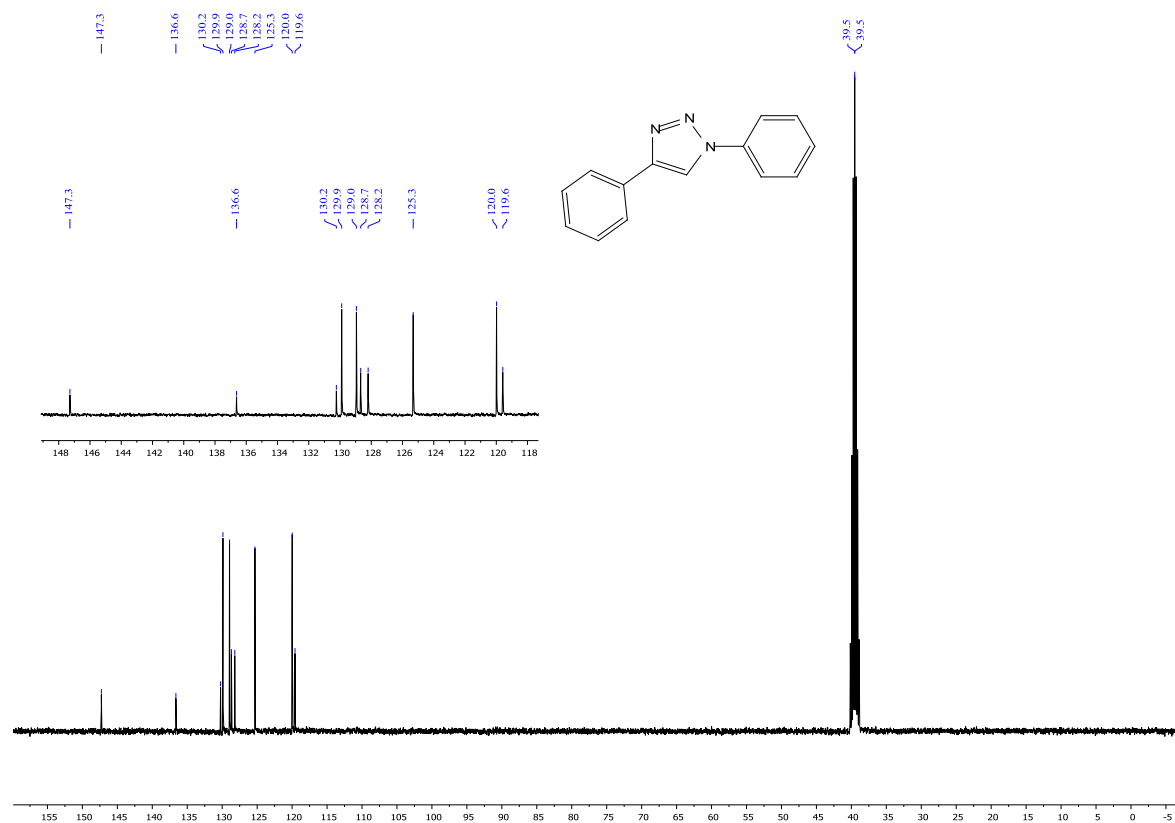


Figure S9. ¹³C NMR (101 MHz, DMSO-*d*₆) spectrum of 1,4-diphenyl-1*H*-1,2,3-triazole (**1**)

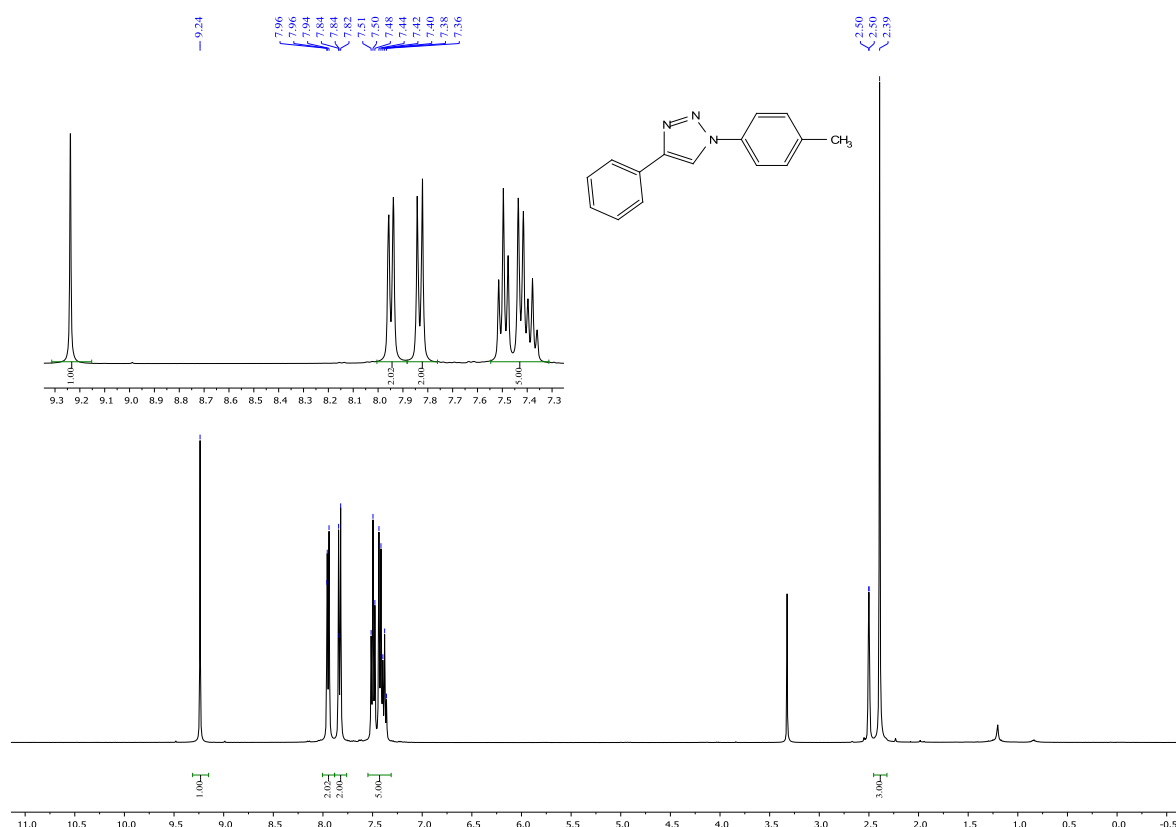


Figure S10. ¹H NMR spectrum (400 MHz, DMSO-*d*₆) of 4-phenyl-1-(*p*-tolyl)-1*H*-1,2,3-triazole (2)

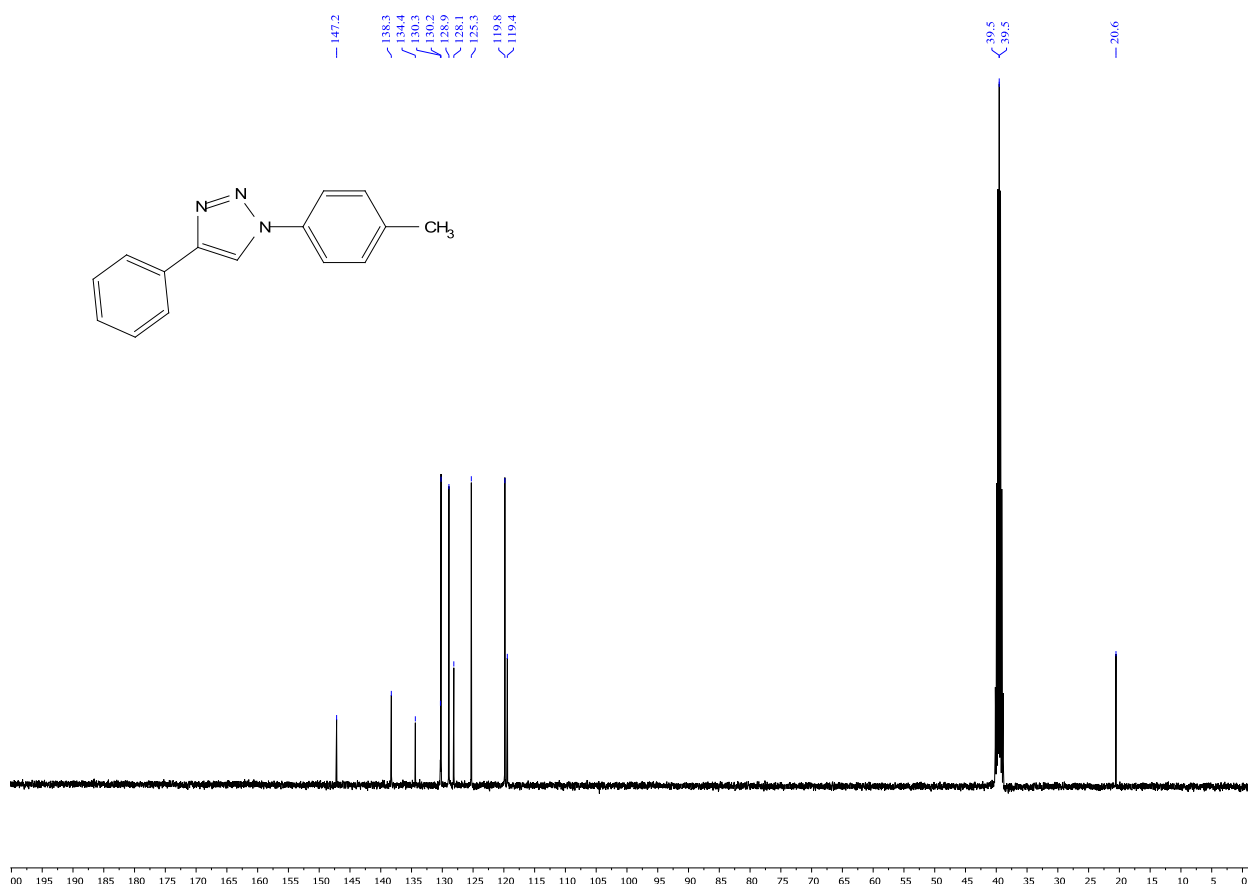


Figure S11. ¹³C NMR (101 MHz, DMSO-*d*₆) spectrum of 4-phenyl-1-(*p*-tolyl)-1*H*-1,2,3-triazole (2)

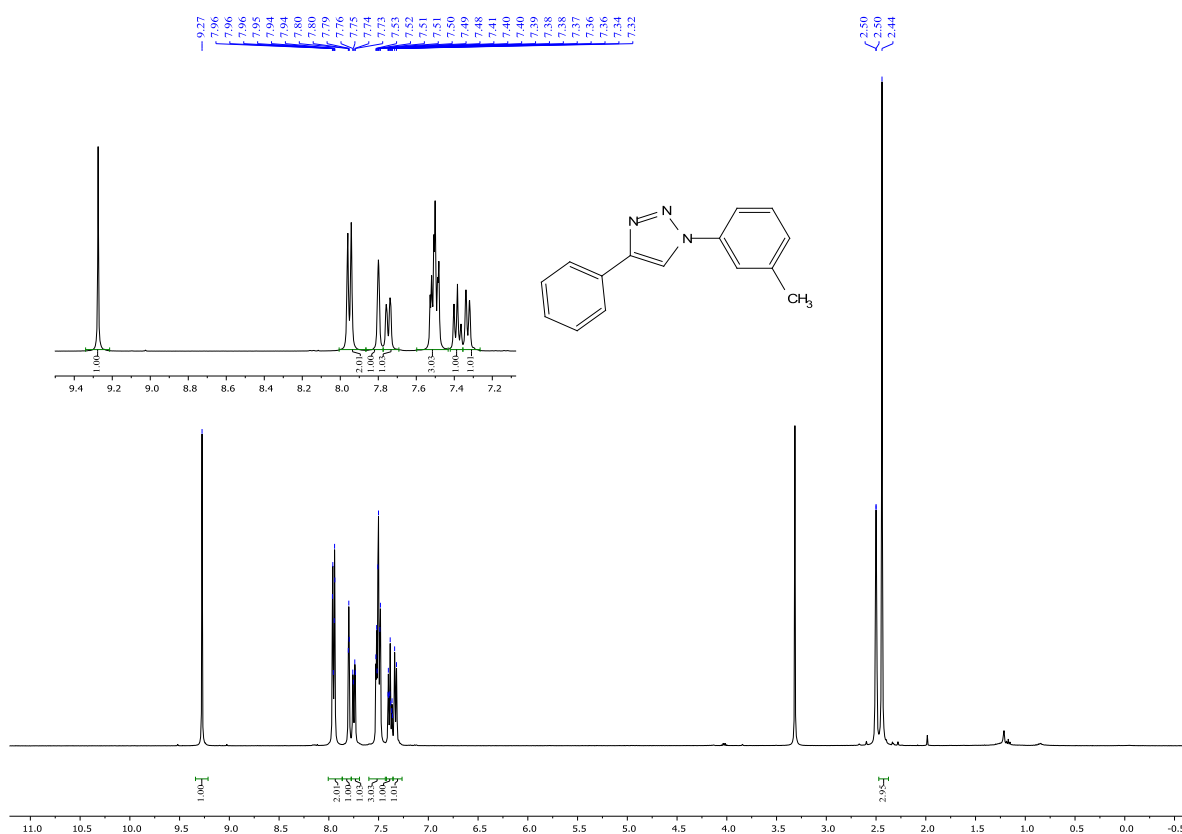


Figure S12. ¹H NMR (400 MHz, DMSO-*d*₆) spectrum of 4-phenyl-1-(*m*-tolyl)-1*H*-1,2,3-triazole (3)

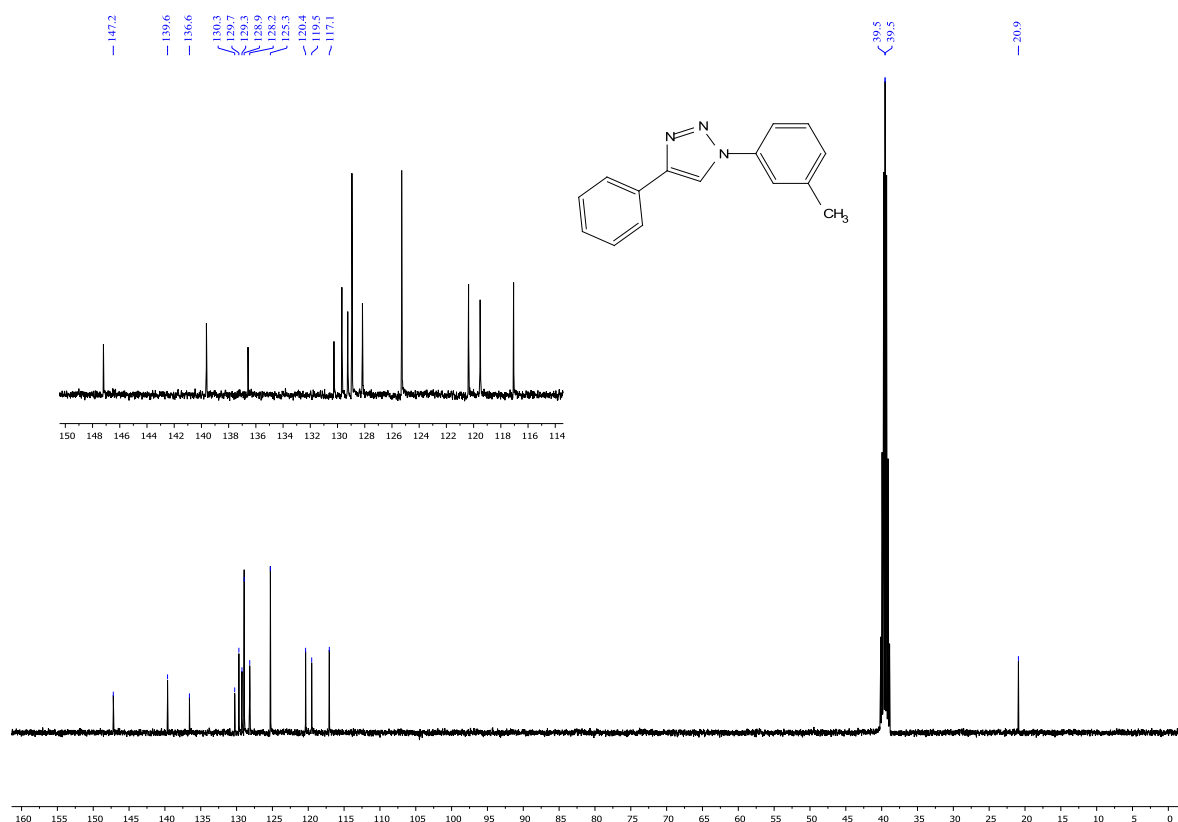


Figure S13. ¹³C NMR (101 MHz, DMSO-*d*₆) spectrum of 4-phenyl-1-(*m*-tolyl)-1*H*-1,2,3-triazole (3)

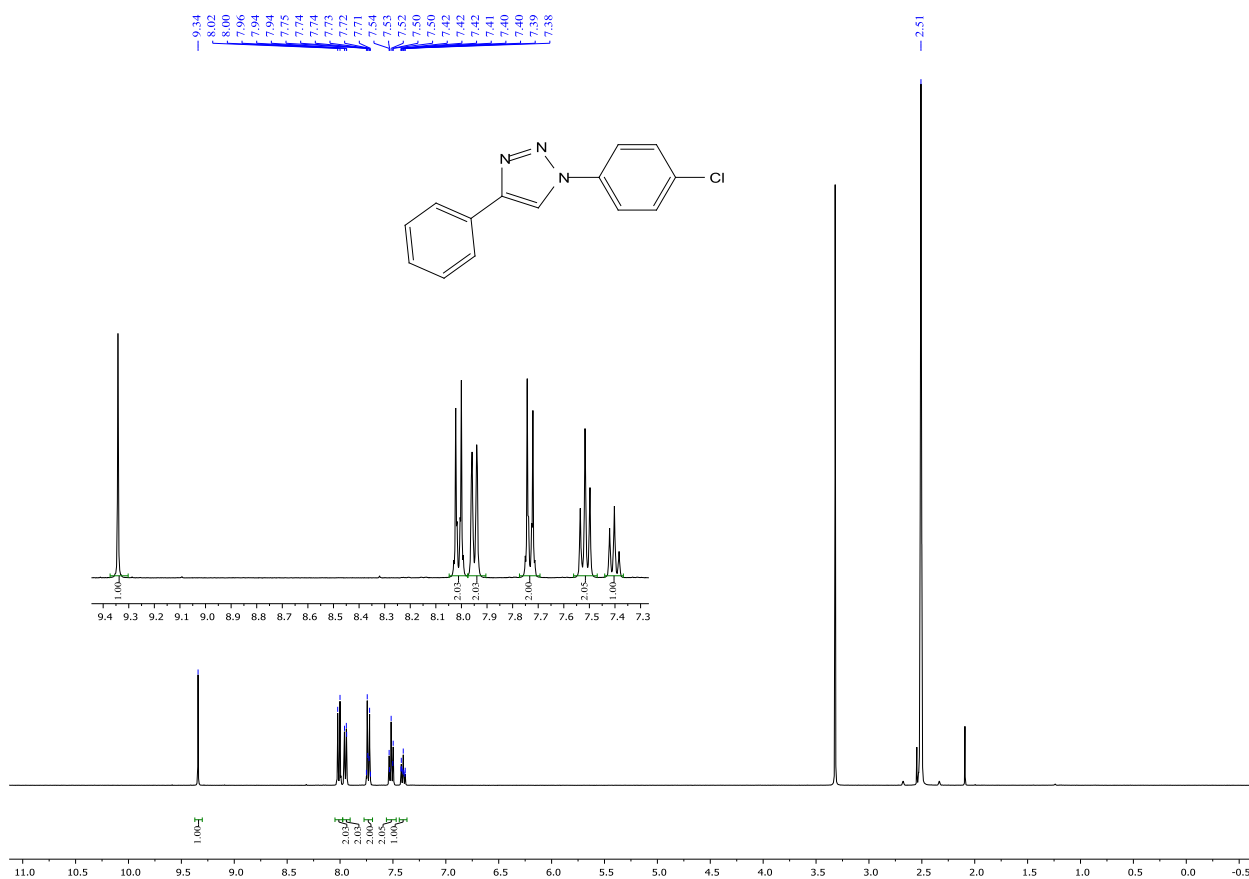


Figure S14. ¹H NMR (400 MHz, DMSO-*d*₆) spectrum of 1-(4-chlorophenyl)-4-phenyl-1*H*-1,2,3-triazol (**4**)

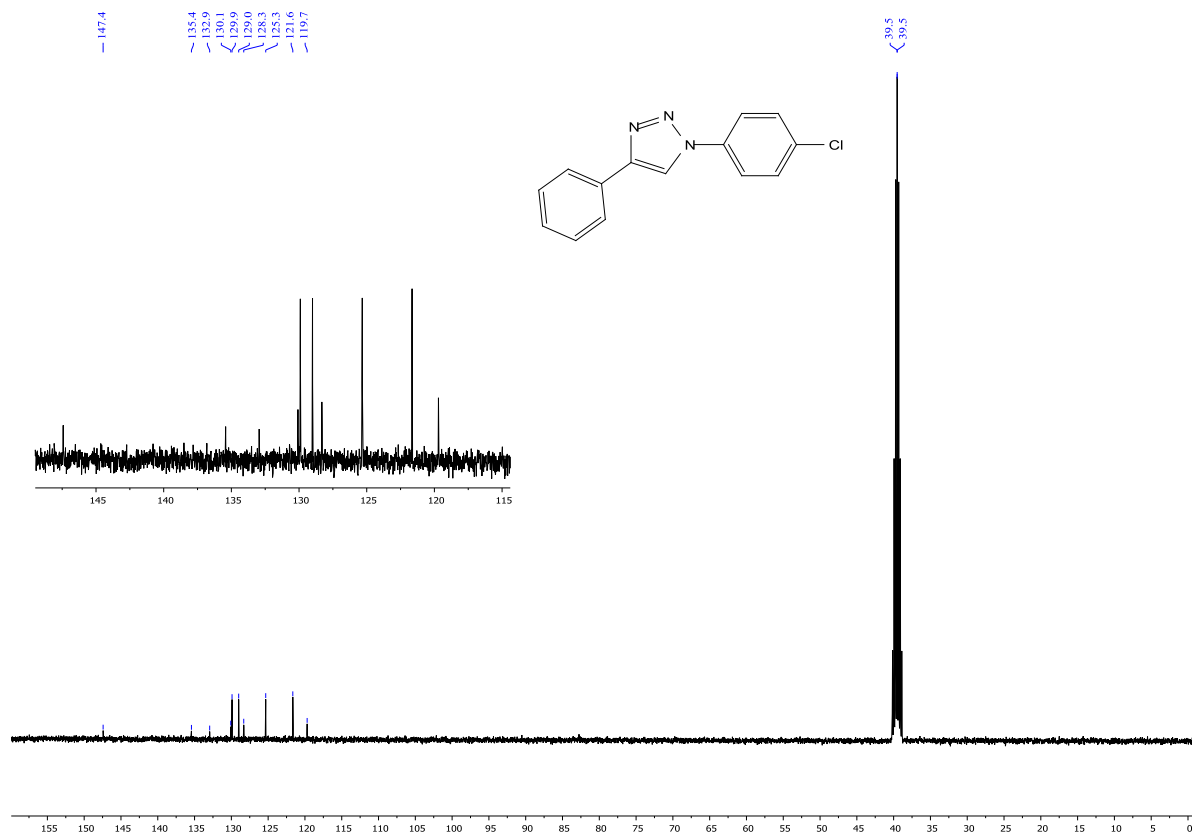


Figure S15. ¹³C NMR (101 MHz, DMSO-*d*₆) spectrum of 1-(4-chlorophenyl)-4-phenyl-1*H*-1,2,3-triazol (**4**)

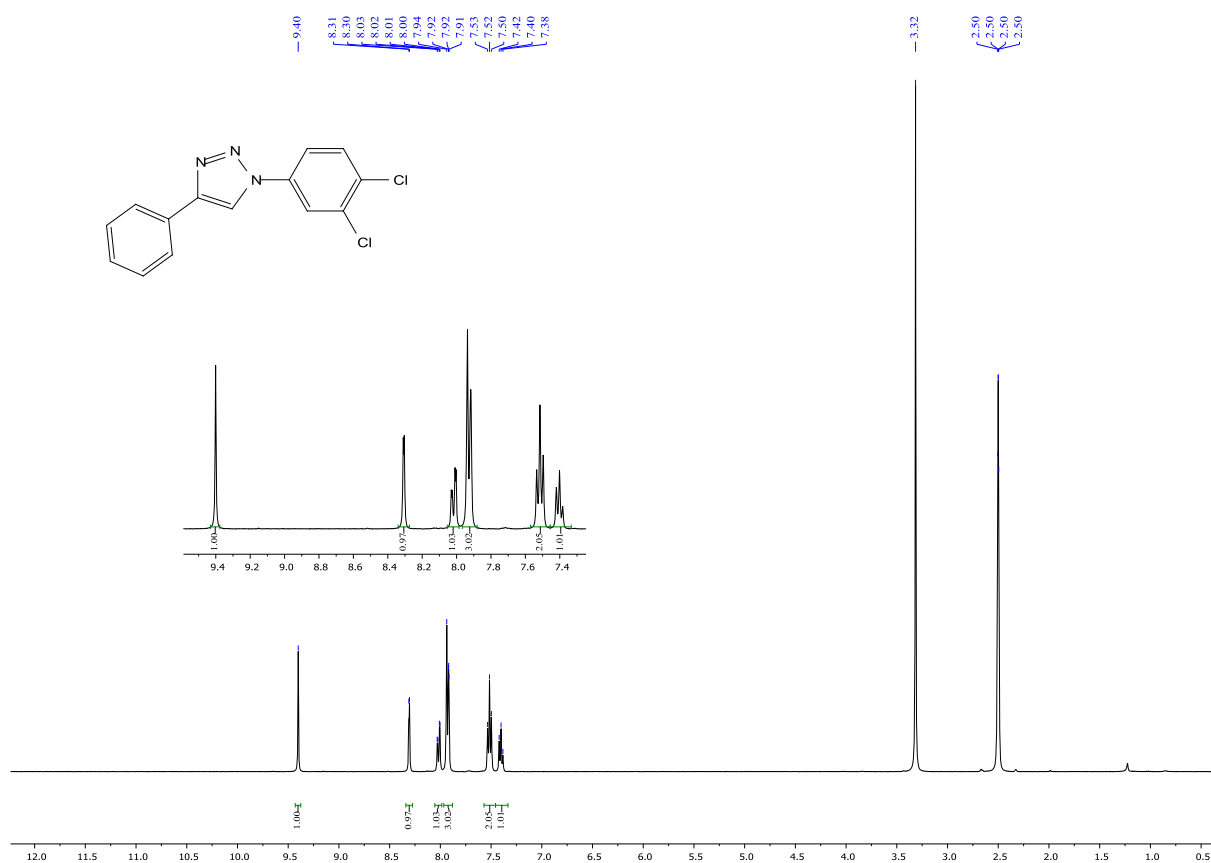


Figure S16. ¹H NMR (400 MHz, DMSO-*d*₆) spectrum of 4-phenyl-1-(3,4-dichlorophenyl)-1*H*-1,2,3-triazole (**5**)

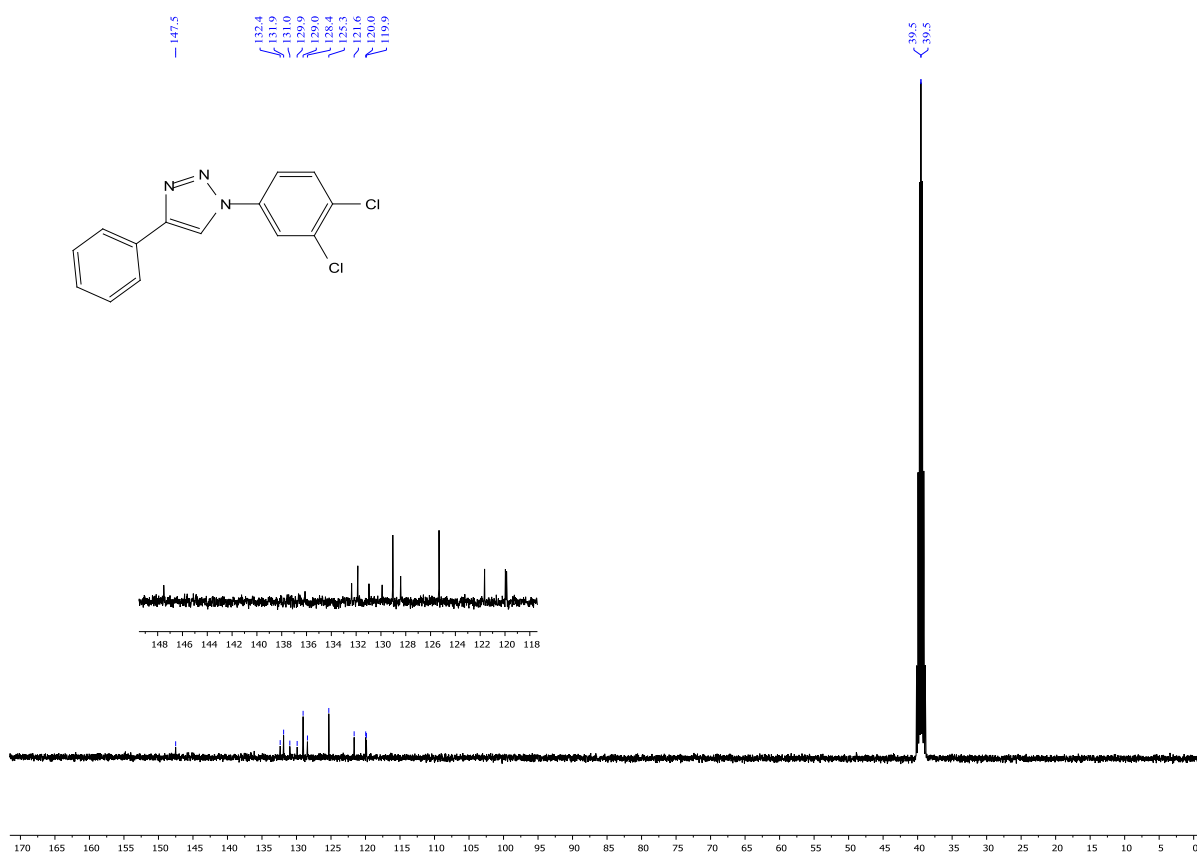


Figure S17. ¹³C NMR (101 MHz, DMSO-*d*₆) spectrum of 4-phenyl-1-(3,4-dichlorophenyl)-1*H*-1,2,3-triazole (**5**)

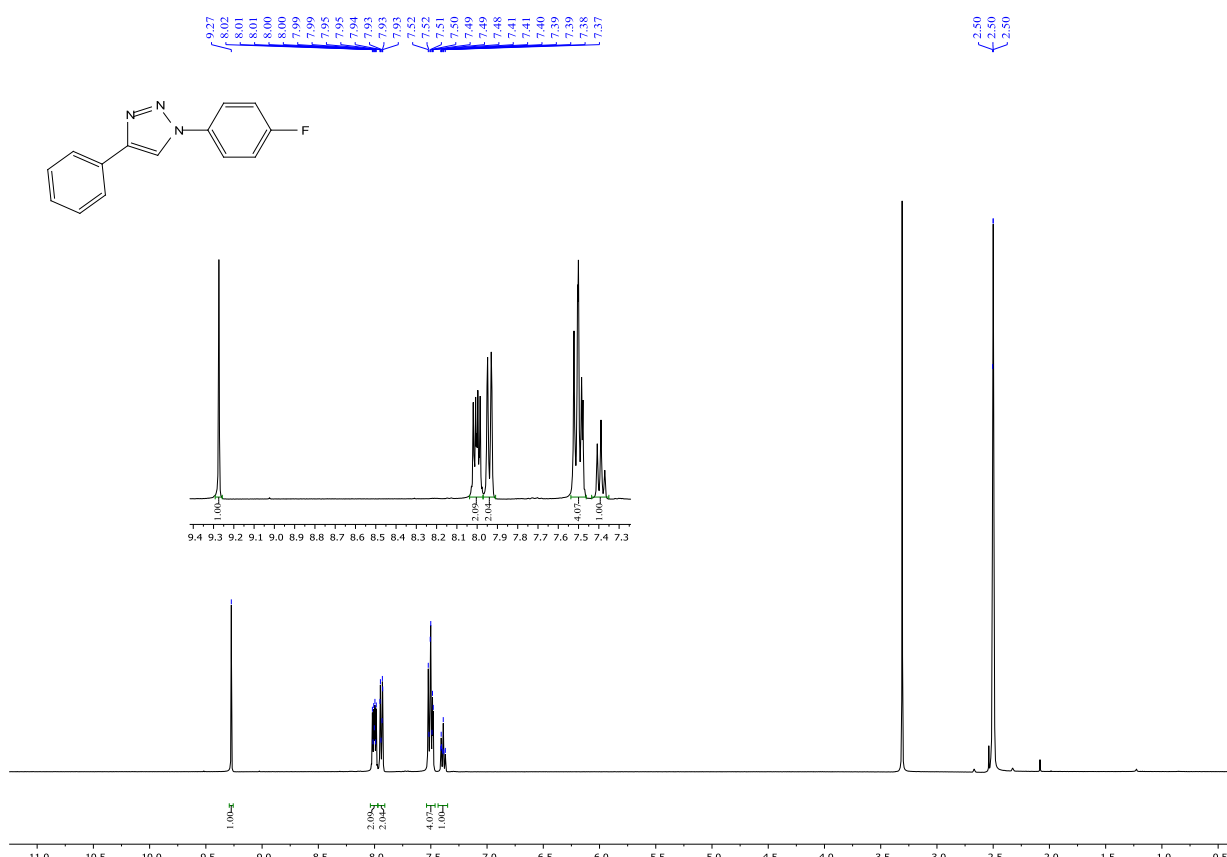


Figure S18. ¹H NMR (400 MHz, DMSO-*d*₆) spectrum of 4-phenyl-1-(4-fluorophenyl)-1*H*-1,2,3-triazole (**6**)

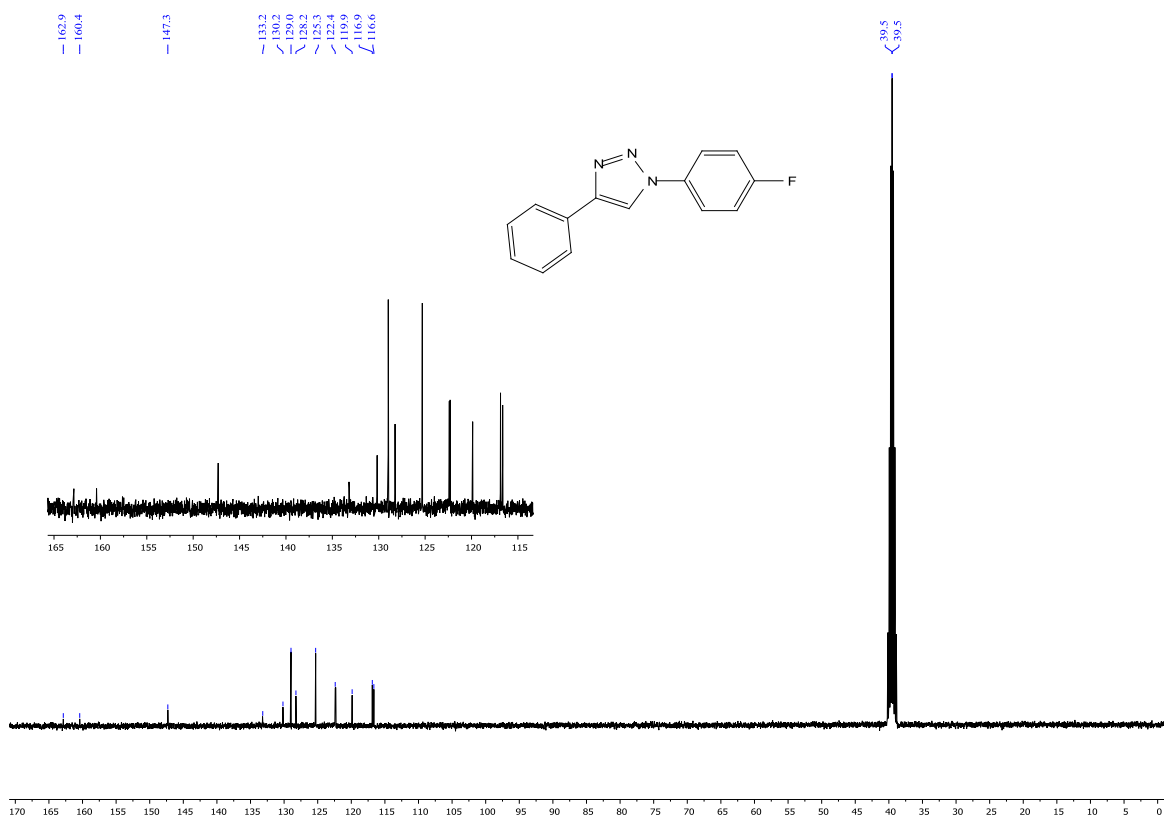


Figure S19. ¹³C NMR (101 MHz, DMSO-*d*₆) spectrum of 4-phenyl-1-(4-fluorophenyl)-1*H*-1,2,3-triazole (**6**)

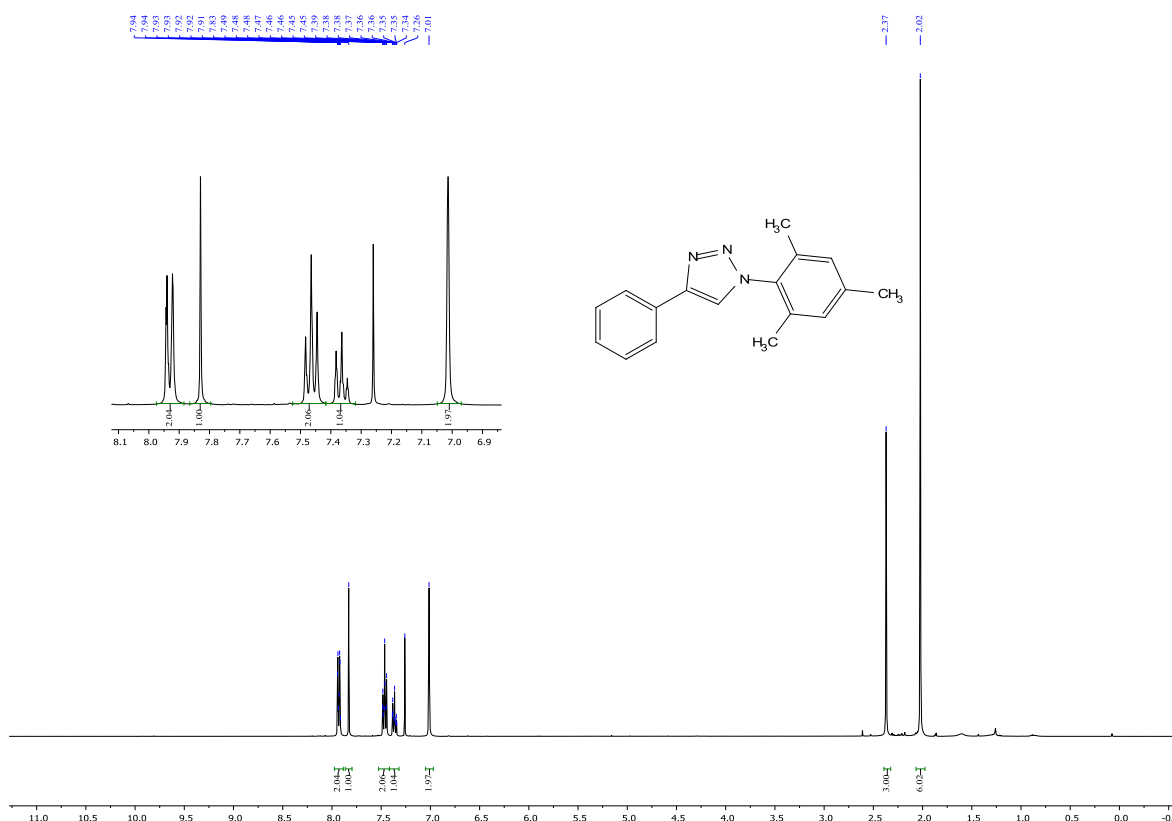


Figure S20. ¹H NMR (400 MHz, CDCl₃) spectrum of 4-phenyl-1-(2,4,6-trimethylphenyl)-1H-1,2,3-triazole (**7**)

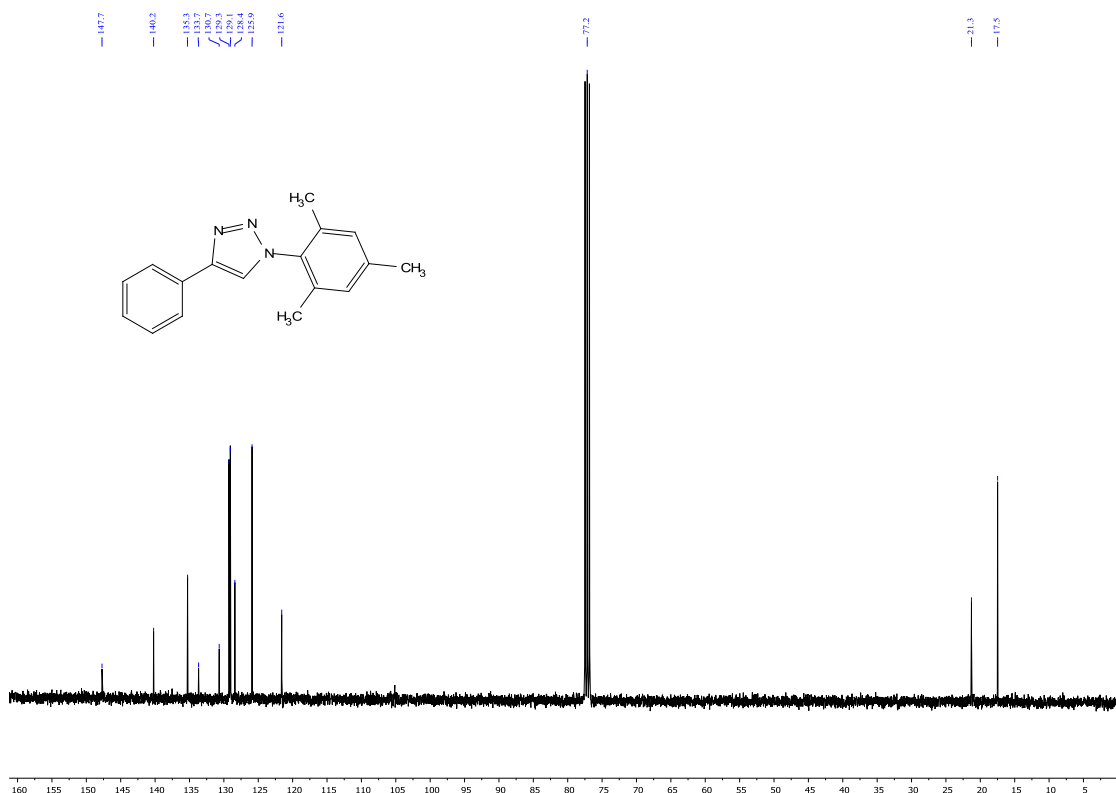


Figure S21. ¹³C NMR (101 MHz, CDCl₃) spectrum of 4-phenyl-1-(2,4,6-trimethylphenyl)-1H-1,2,3-triazole (**7**)

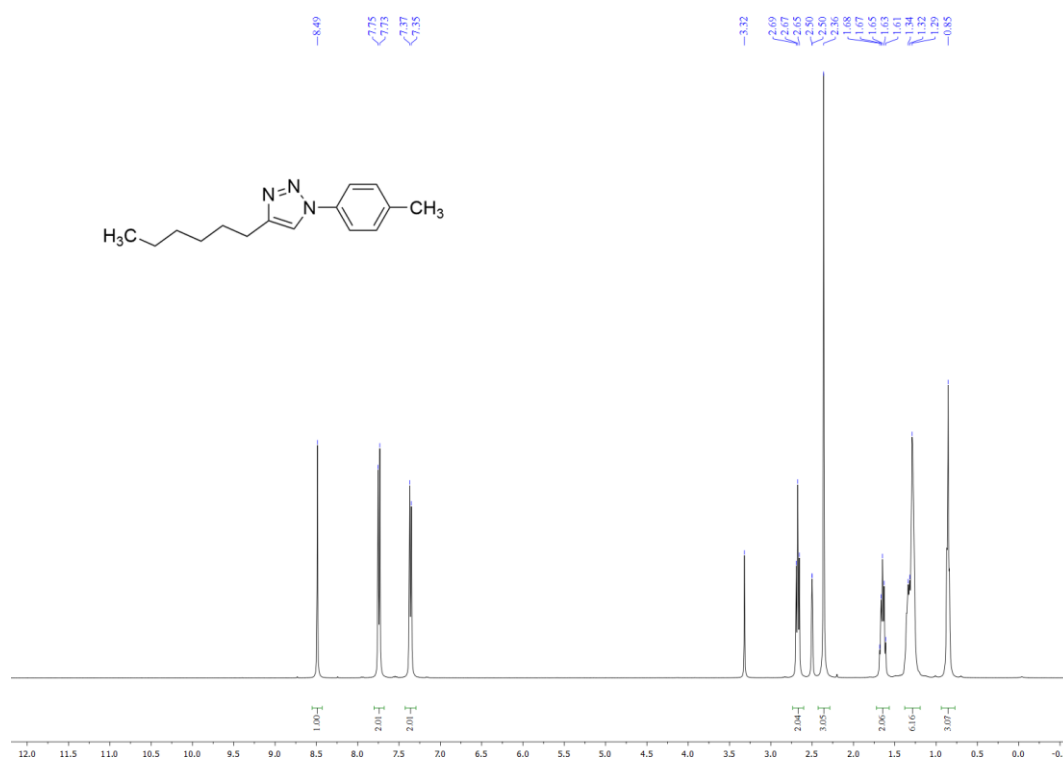


Figure S24. ¹H NMR (400 MHz, DMSO-*d*₆) spectrum of 4-*n*-hexyl-1-(*p*-tolyl)-1*H*-1,2,3-triazole (9)

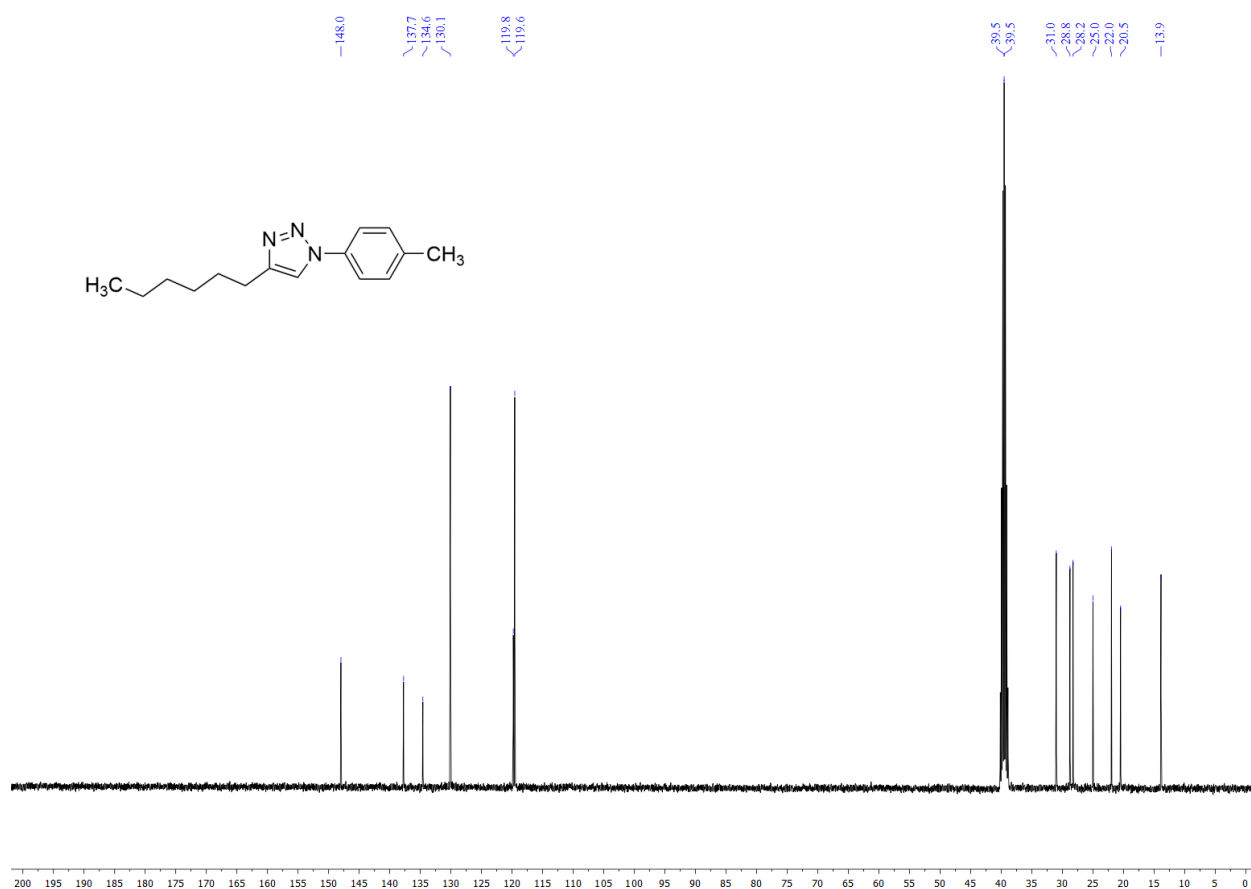


Figure S25. ¹³C NMR (101 MHz, DMSO-*d*₆) spectrum of 4-*n*-hexyl-1-(*p*-tolyl)-1*H*-1,2,3-triazole (9)

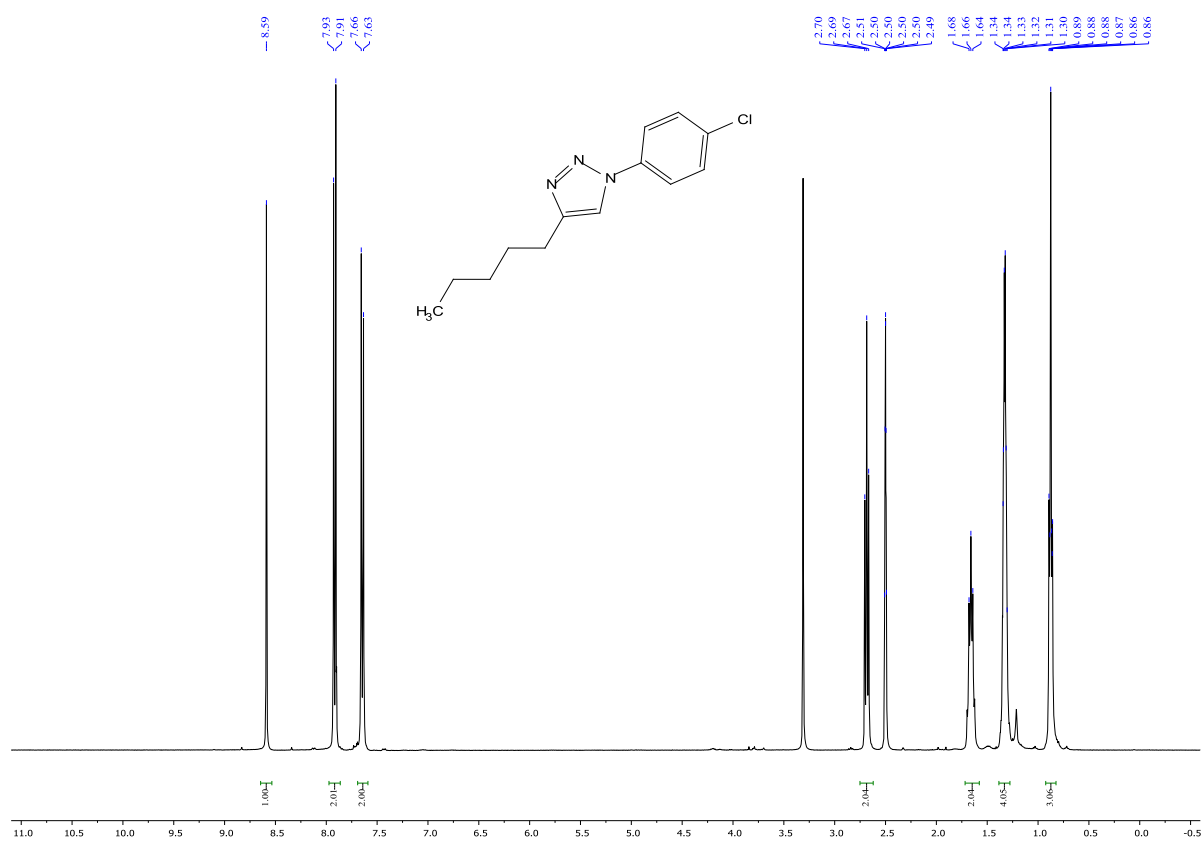


Figure S26. ¹H NMR (400 MHz, DMSO-*d*₆) spectrum of 1-(4-chlorophenyl)-4-n-pentyl-1H-1,2,3-triazole (10)

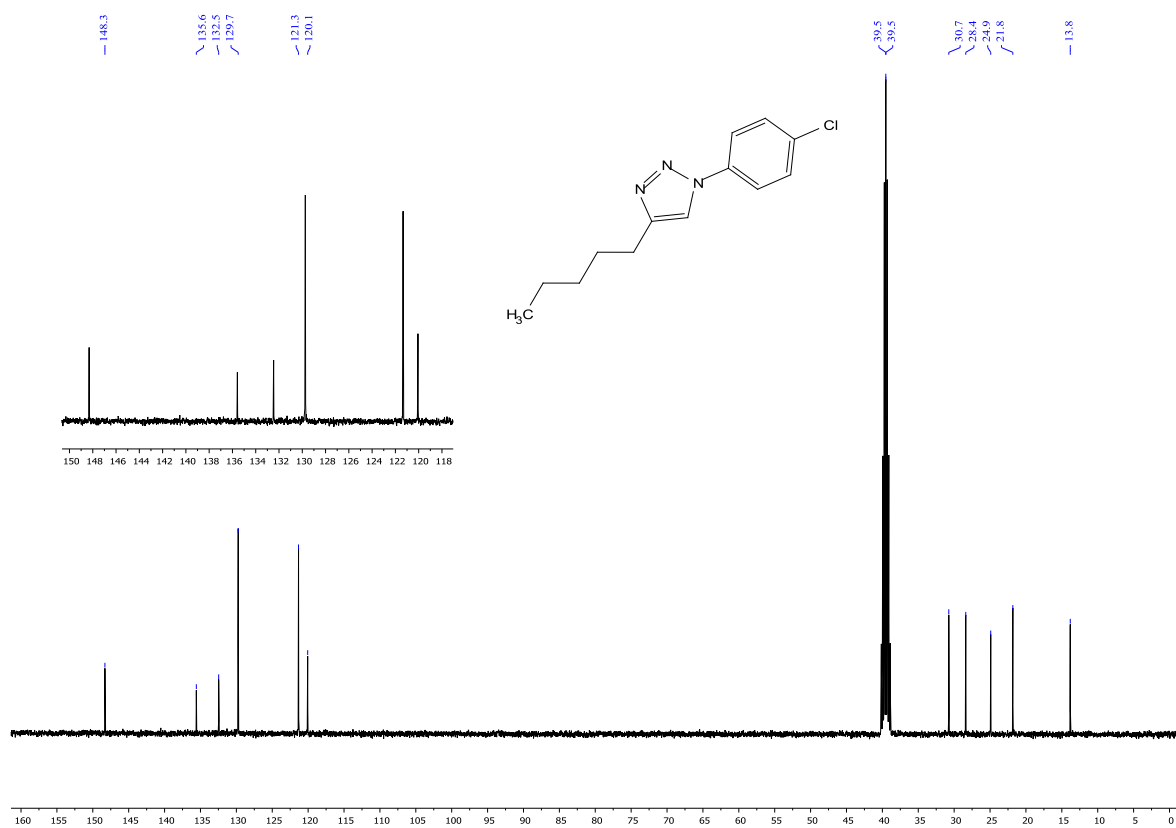


Figure S27. ¹³C NMR (101 MHz, DMSO-*d*₆) spectrum of 1-(4-chlorophenyl)-4-n-pentyl-1H-1,2,3-triazole (10)

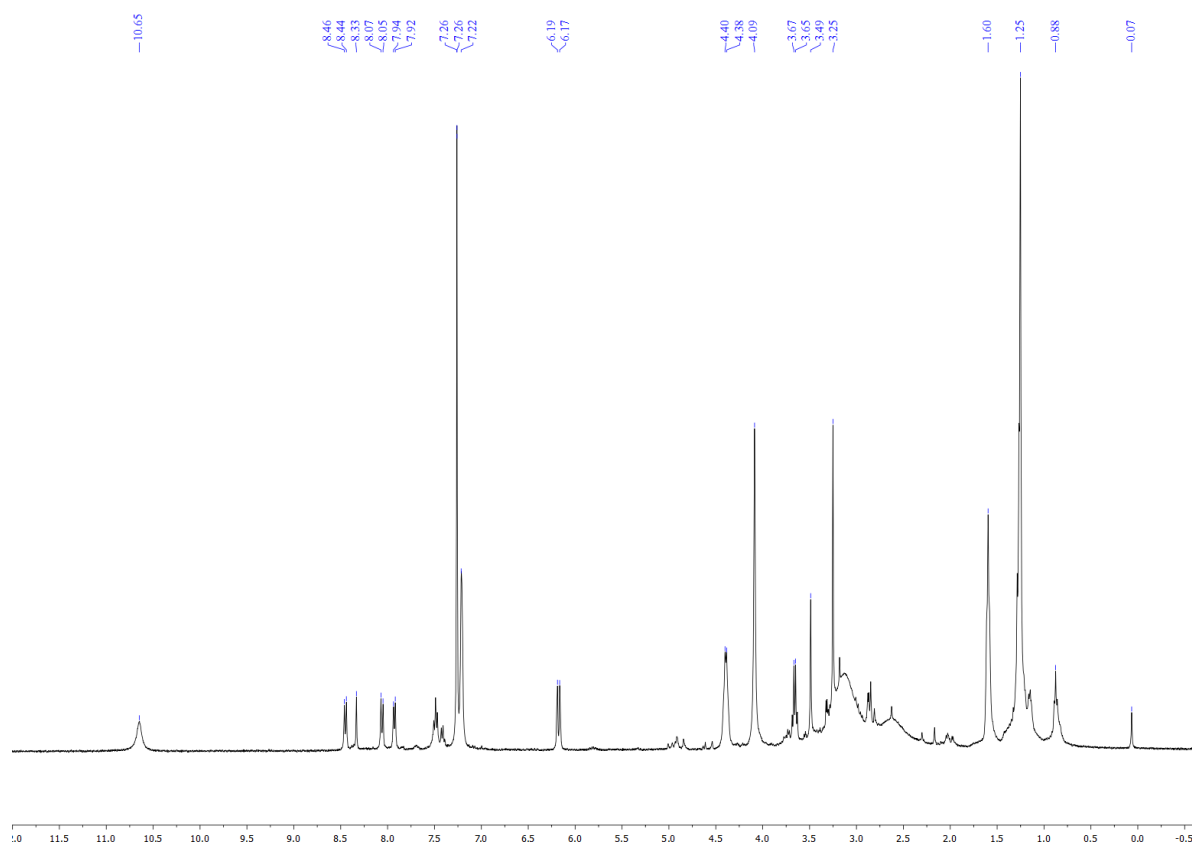


Figure S28. ¹H NMR (400 MHz, CDCl₃) spectrum of 1-(4-nitrophenyl)-1H-1,2,3-triazole (**11**) after column chromatography (with some impurities from the reaction mixture; see the text).

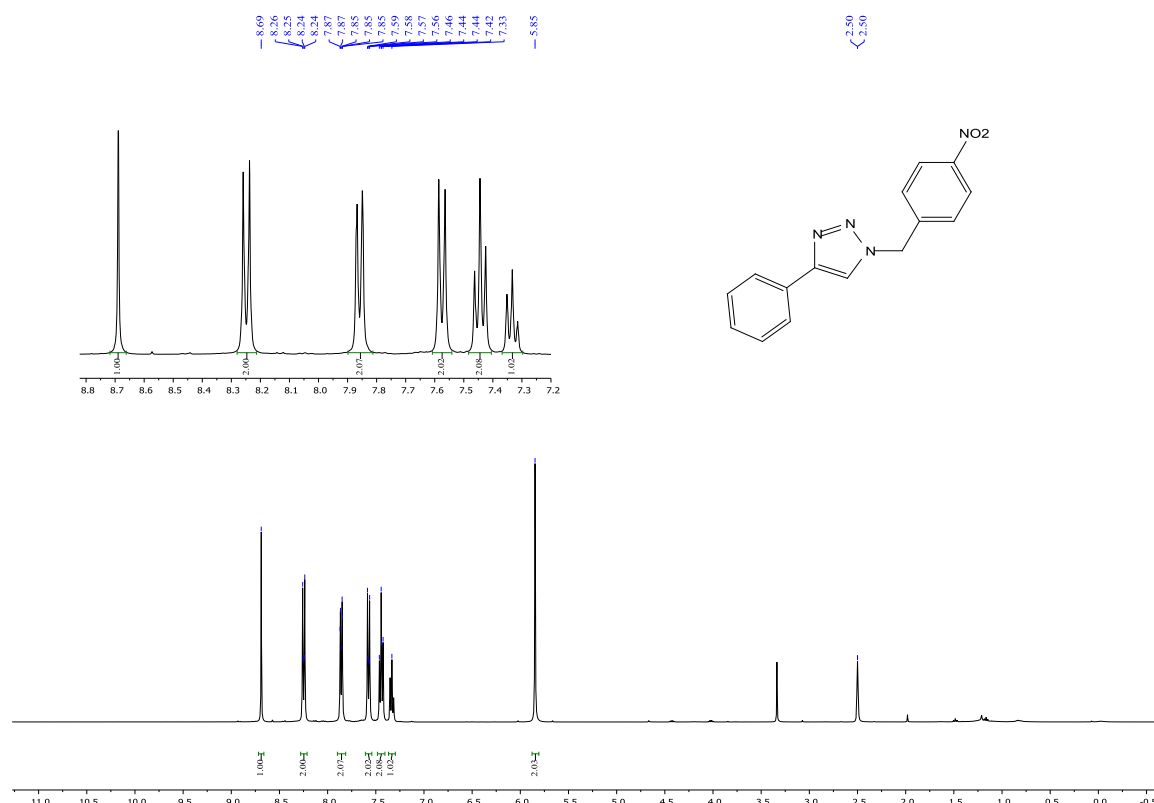


Figure S29. ¹H NMR (400 MHz, DMSO-*d*₆) spectrum of 1-(4-nitrobenzyl)-4-phenyl-1H-1,2,3-triazole (**12**)

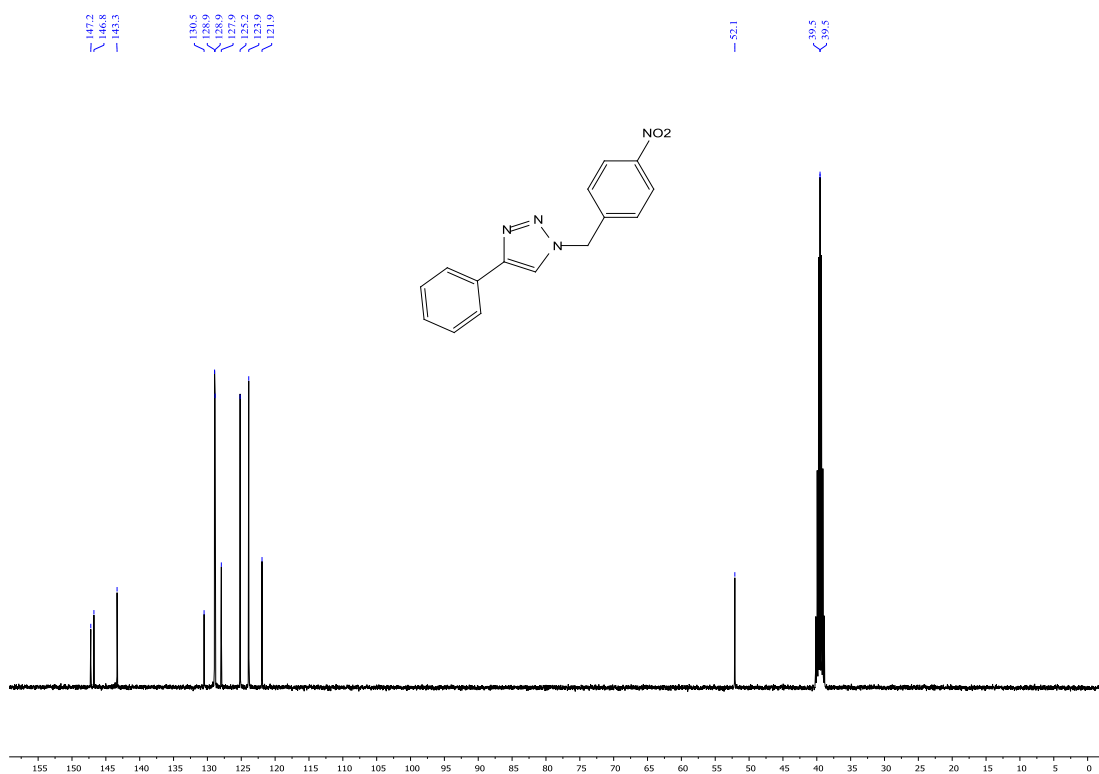


Figure S30. ¹³C NMR (101 MHz, DMSO-*d*₆) spectrum of 4-phenyl-1-(4-nitrobenzyl)-1*H*-1,2,3-triazole (**12**)

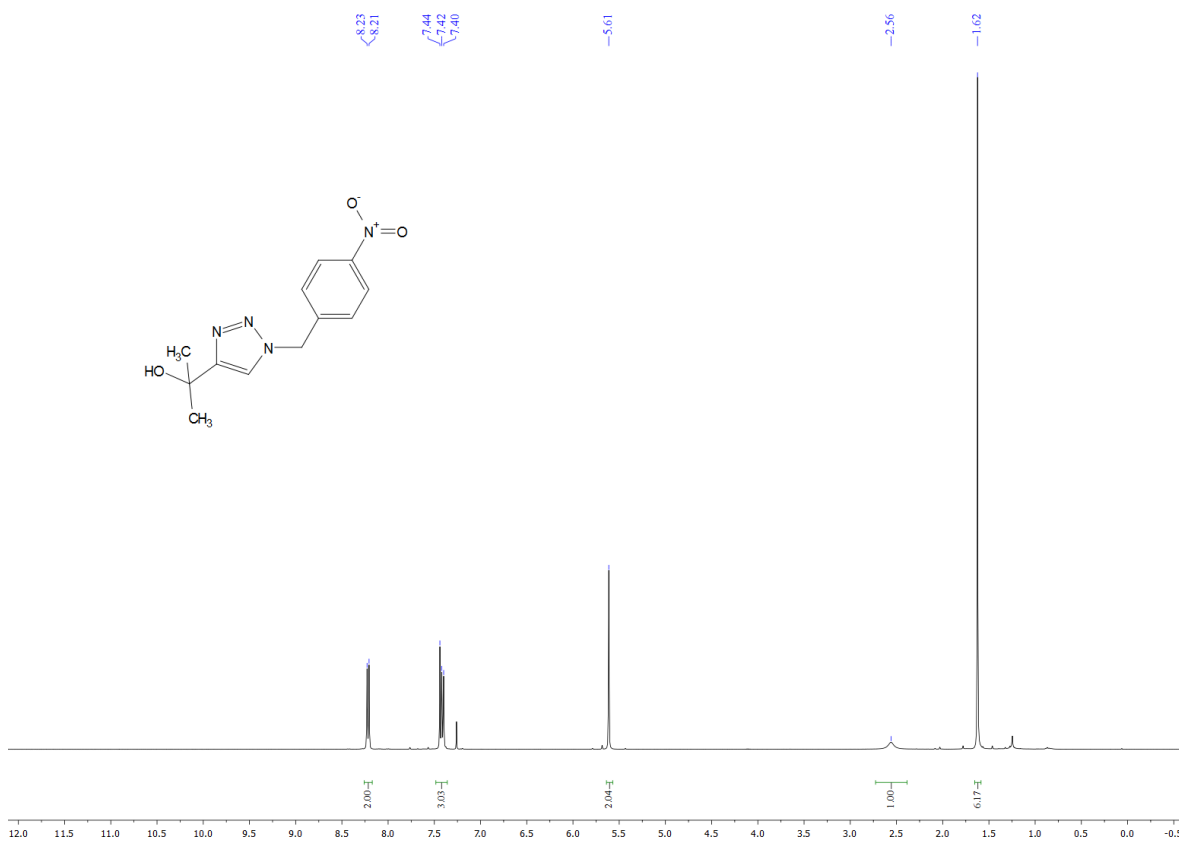


Figure S31. ¹H NMR (400 MHz, CDCl₃) spectrum of 2-(1-(4-nitrobenzyl)-1*H*-1,2,3-triazol-4-yl)propan-2-ol (**13**)

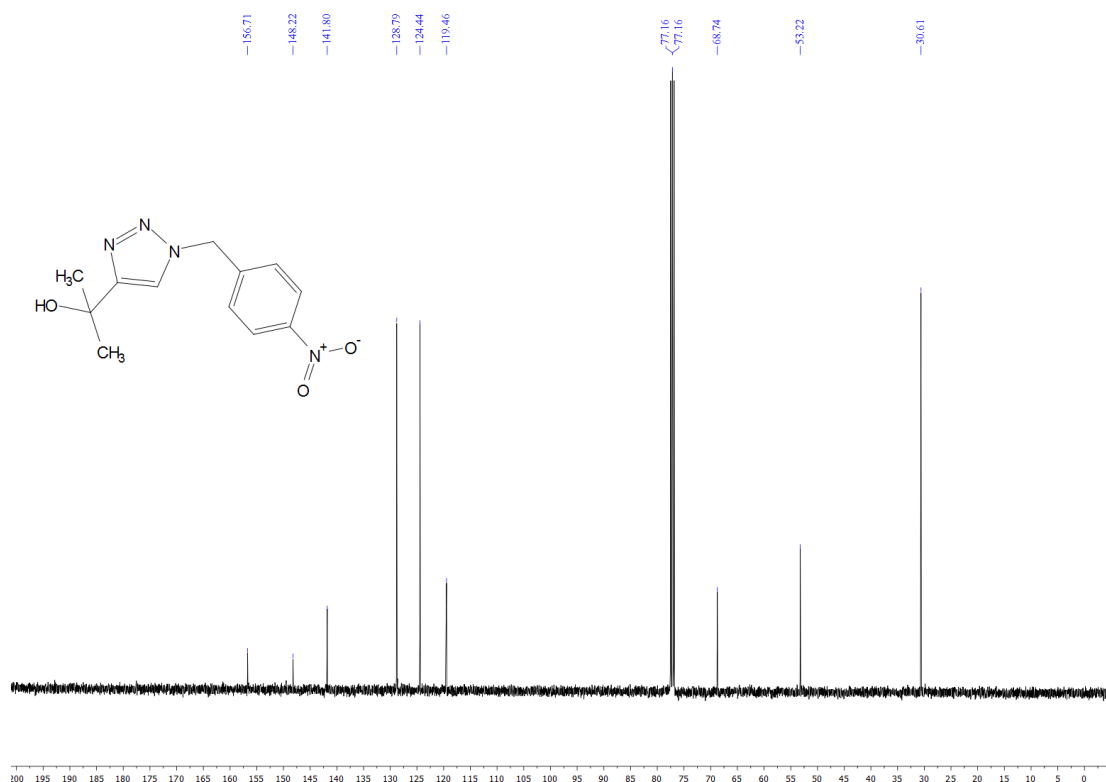


Figure S32. ¹³C NMR (101 MHz, CDCl₃) spectrum of 2-(1-(4-nitrobenzyl)-1H-1,2,3-triazol-4-yl)propan-2-ol (13)

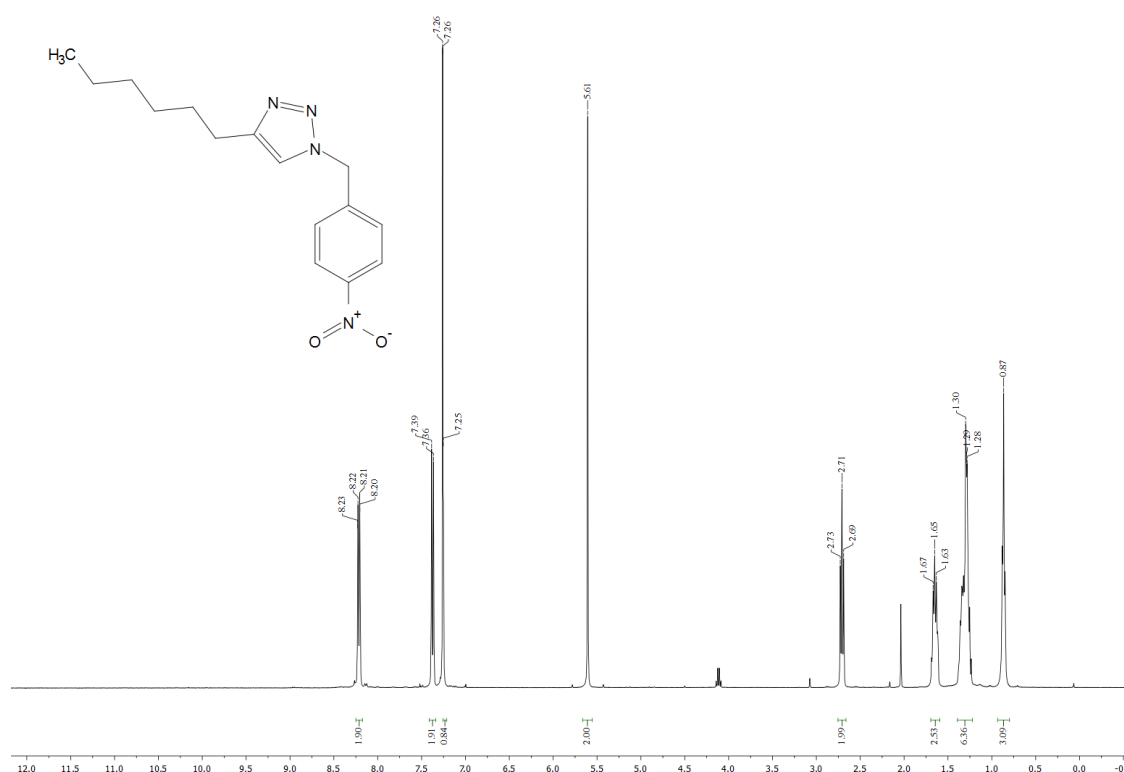


Figure S33. ¹H NMR (400 MHz, CDCl₃) spectrum of 1-(4-nitrobenzyl)-4-hexyl-1H-1,2,3-triazole (14)

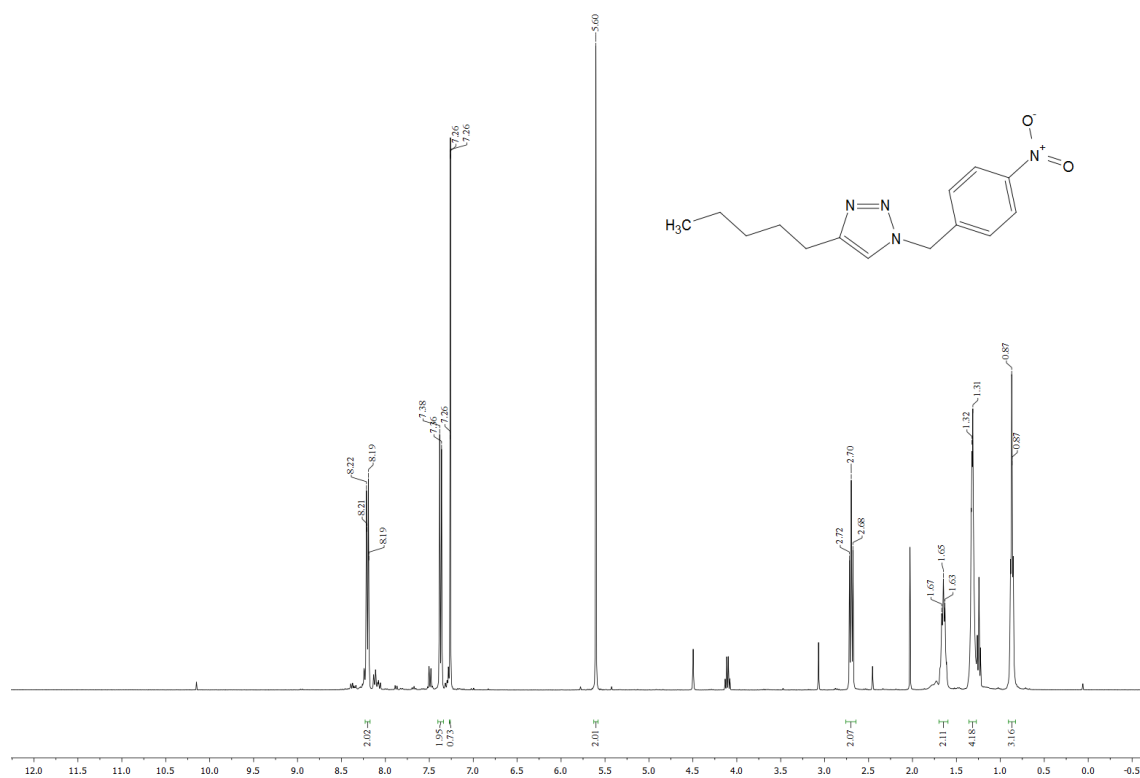


Figure S34. ¹H NMR (400 MHz, CDCl₃) spectrum of 1-(4-nitrobenzyl)-4-pentyl-1H-1,2,3-triazole (**15**)

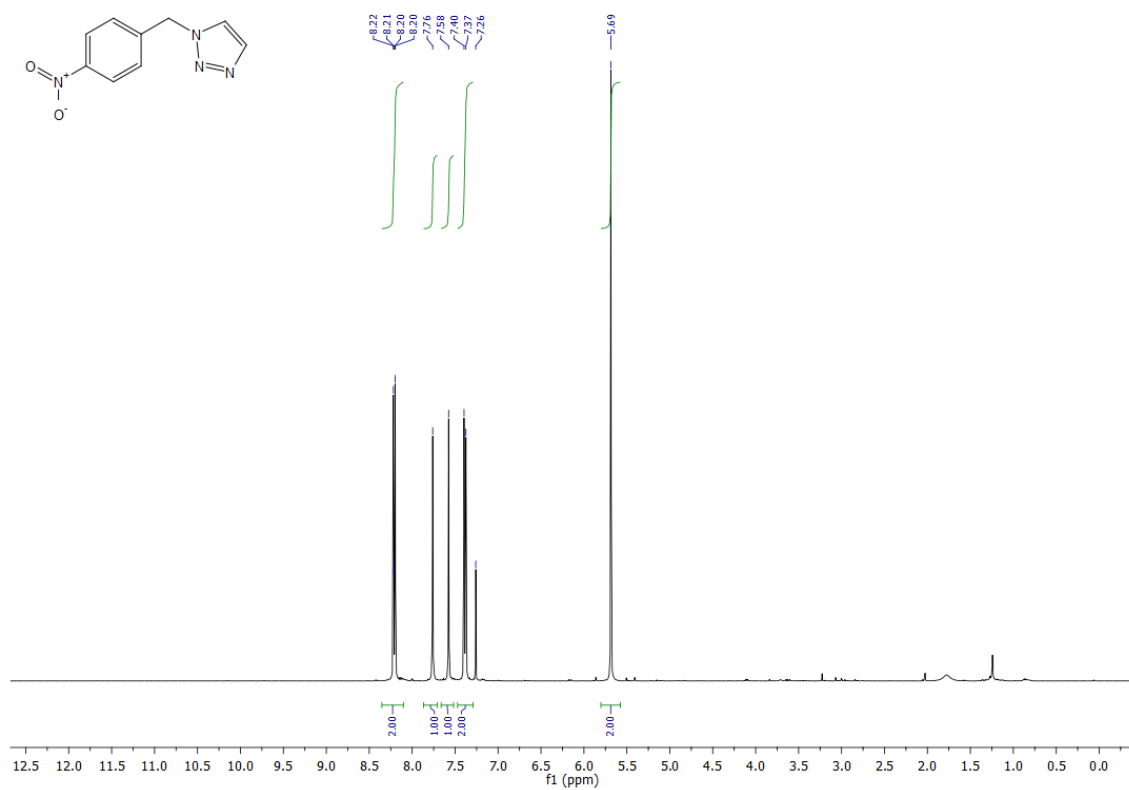


Figure S35. ¹H NMR (400 MHz, CDCl₃) spectrum of 1-(4-nitrobenzyl)-1H-1,2,3-triazole (**16**).

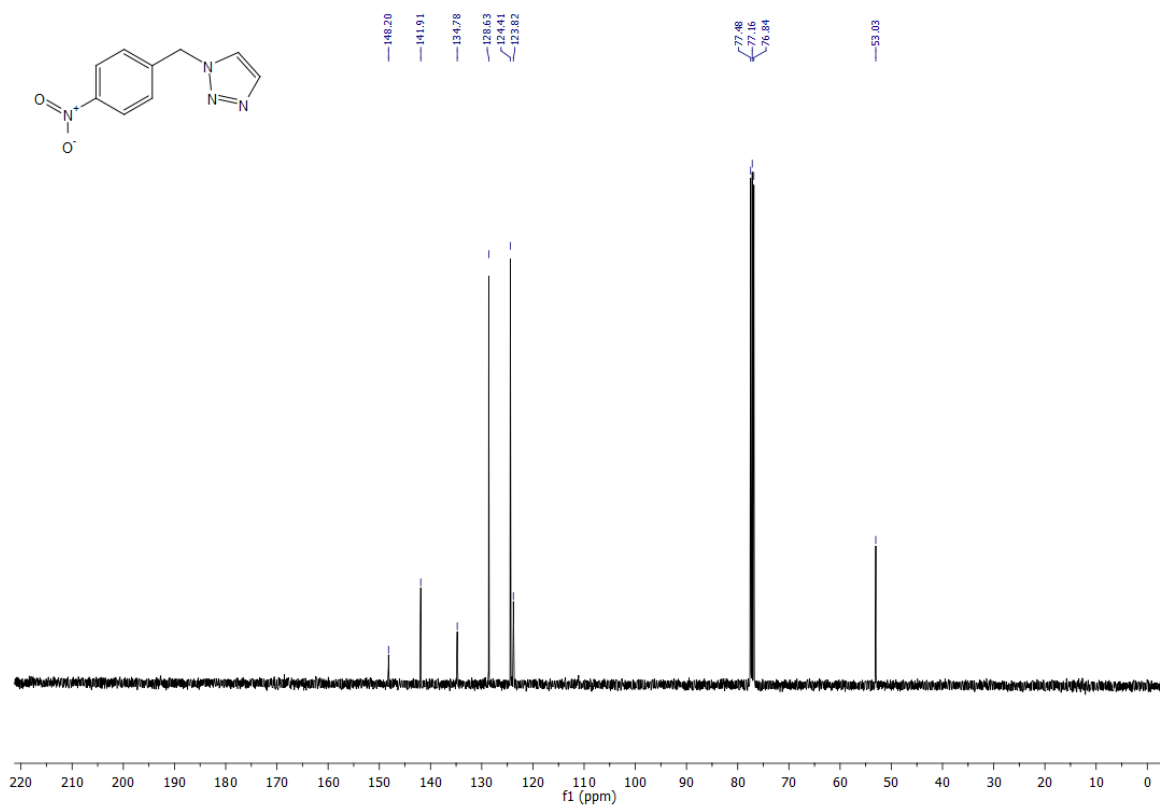


Figure S36. ^{13}C NMR (101 MHz, CDCl_3) spectrum of 1-(4-nitrobenzyl)-1H-1,2,3-triazole (**16**).

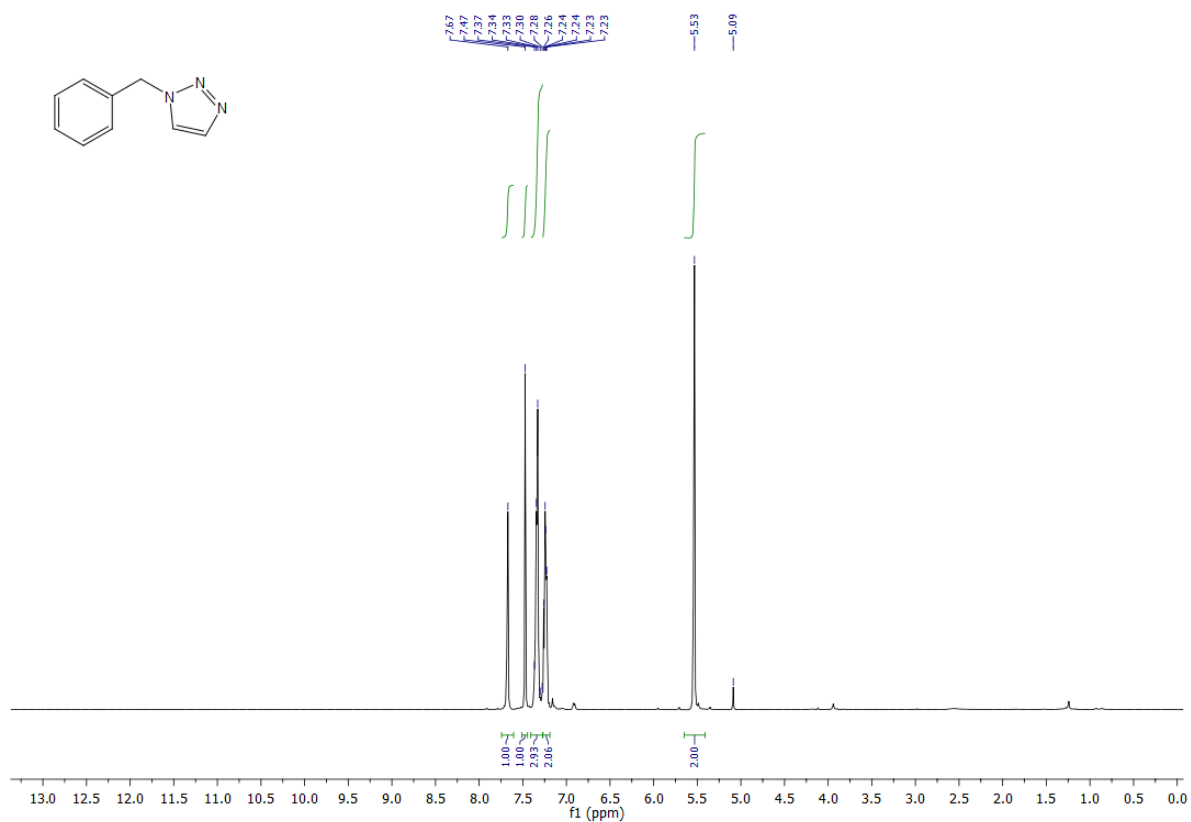


Figure S37. ^1H NMR (400 MHz, CDCl_3) spectrum of 1-benzyl-1H-1,2,3-triazole (**17**).

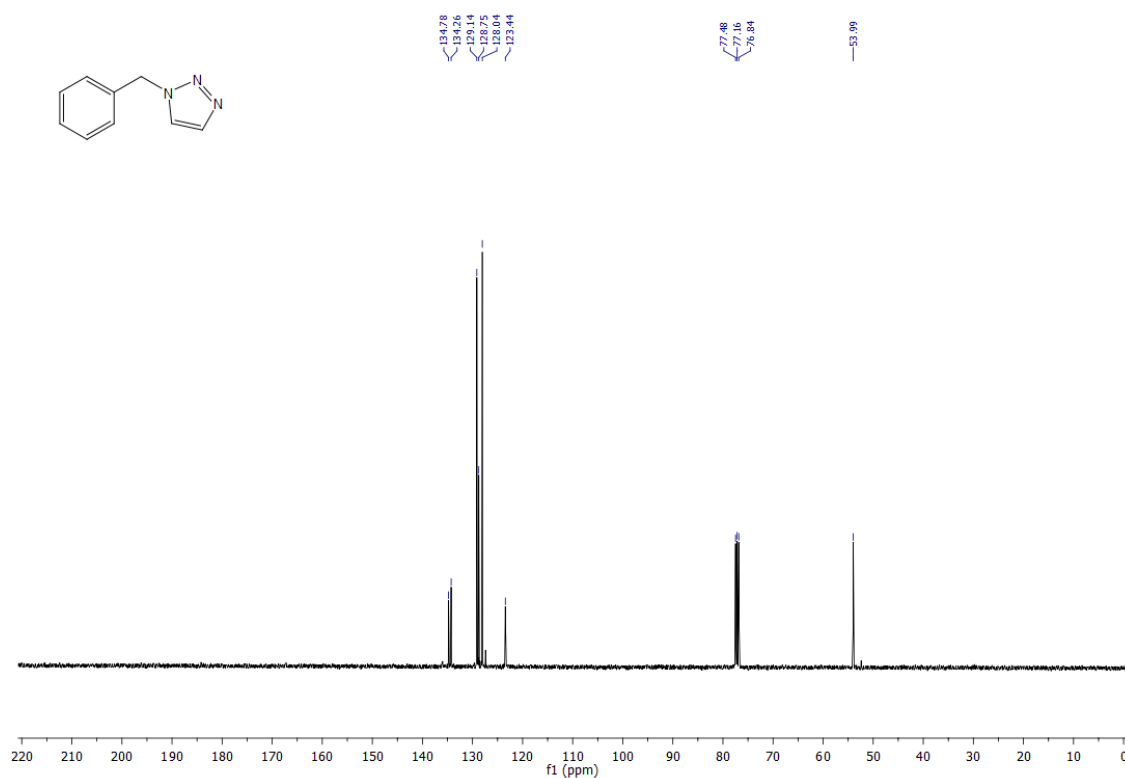


Figure S38. ^{13}C NMR (101 MHz, CDCl_3) spectrum of 1-benzyl-1H-1,2,3-triazole (**17**).

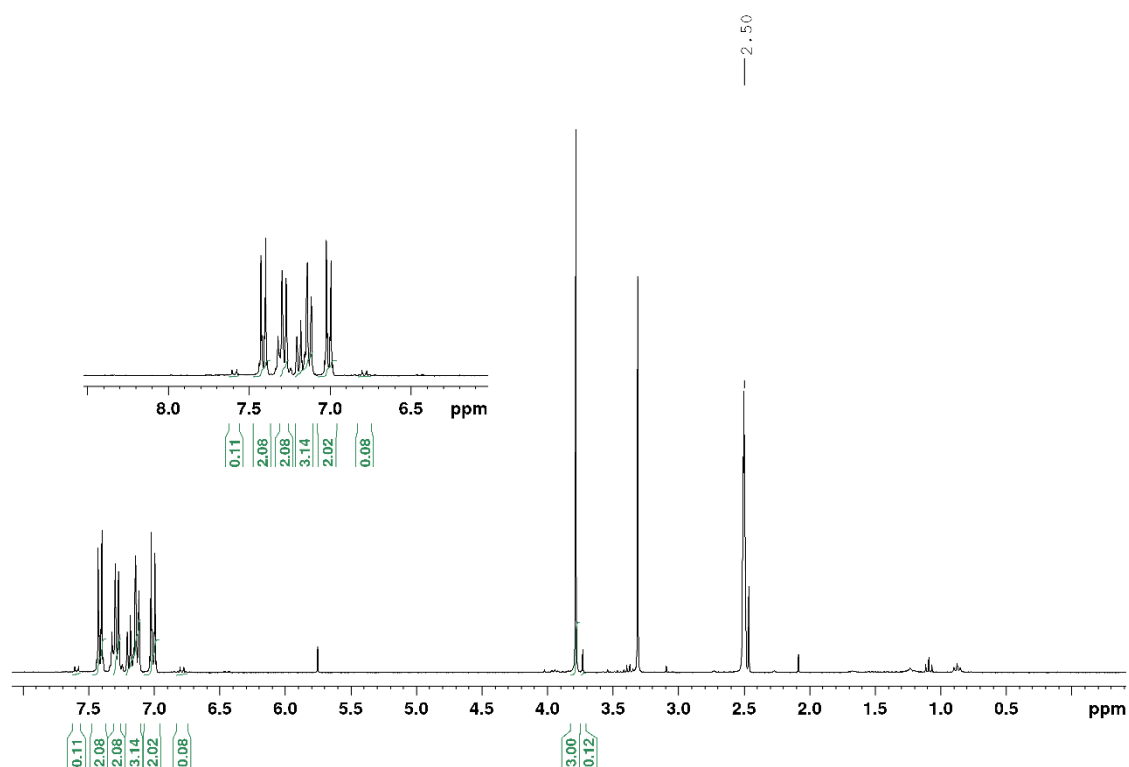


Figure S39. ^1H NMR (300 MHz, $\text{DMSO}-d_6$) spectrum of the reaction mixture after C-S cross-coupling between thiophenol and 4-iodanisole, extracted from IL medium (**18**). Residual water appears as a singlet at 3.31 ppm.

S5. XRD data

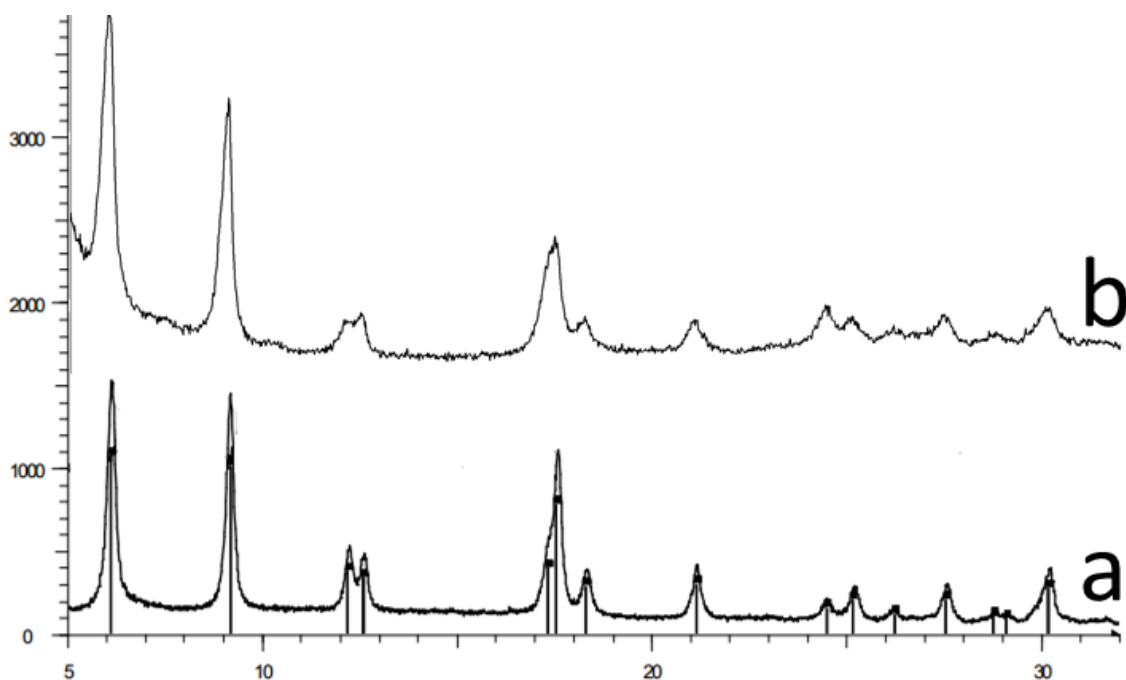


Figure S40. XRD data of copper phenylacetylenide at literature source (a) and this work (b)

Table S6: XRD data for copper phenylacetylenide obtained

No.	2-theta(deg)	d(ang.)
1	6.068(5)	14.554(12)
2	9.120(5)	9.689(5)
3	12.15(2)	7.281(14)
4	12.535(12)	7.056(7)
5	17.500(8)	5.064(2)
6	18.245(15)	4.859(4)
7	21.02(2)	4.223(4)
8	24.42(2)	3.642(3)
9	25.05(3)	3.552(4)
10	26.12(5)	3.409(6)
11	26.74(11)	3.331(14)
12	27.45(2)	3.246(2)
13	28.81(5)	3.096(5)
14	30.12(3)	2.964(2)

S6. SEM data

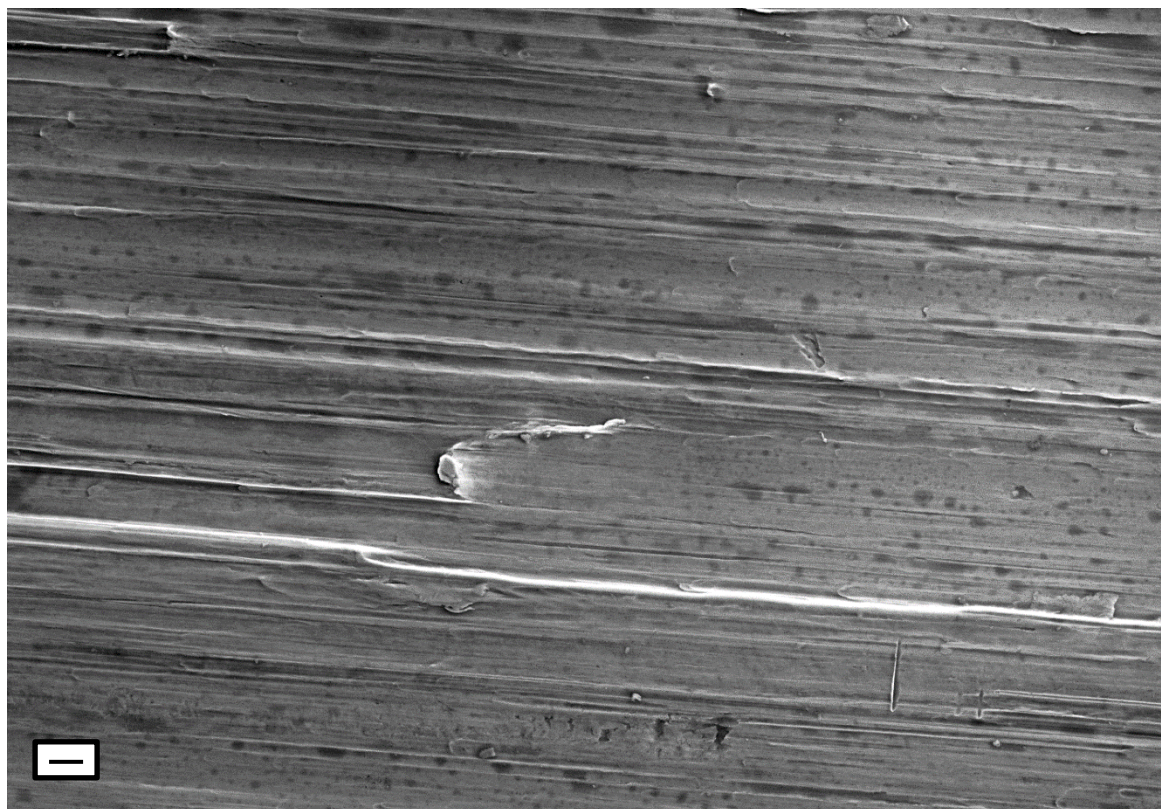


Figure S41. SEM image of a copper electrode after treatment with HCl and electrochemical dissolution. Scale bar 20 μm .

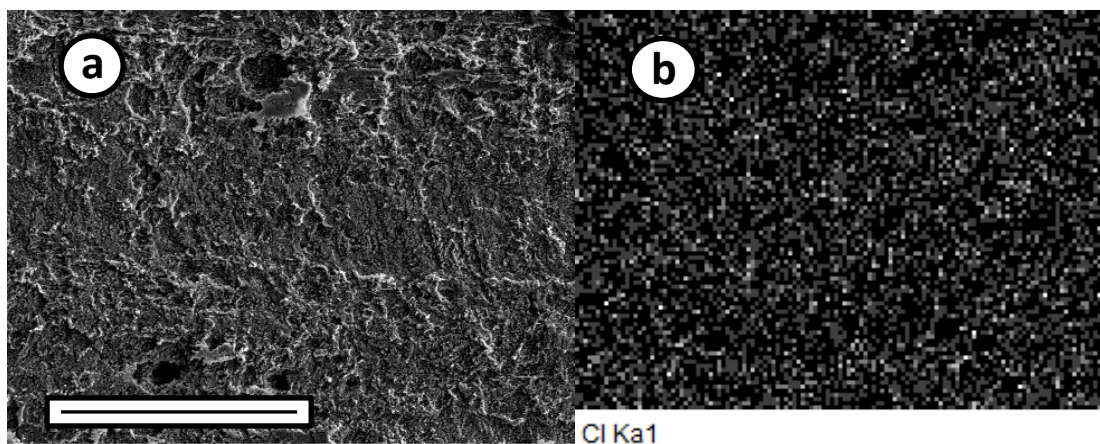


Figure S42. SEM image of a copper electrode after treatment with HCl and electrochemical dissolution process (a), scale bar 30 μm ; EDS chlorine atoms map on the same copper electrode surface (b).

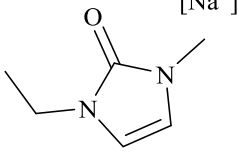
Table S7. Elemental analysis of the copper electrode surface (Figure S42, a).

Elemental analysis	O, %	Si, %	Cl, %	Cu, %	Total, mas.%
	1.28	0.10	0.04	98.58	100.00

The presence of oxygen in the sample can be explained by the oxidation of copper from the electrode surface with atmospheric oxygen. The presence of silicon is possible as a result of mechanical treatment of the original electrode with an abrasive.

S7. HRESI-MS data

Table S8. HRESI-MS data.

Structure	Formula	[M] ⁺ (found)	[M] ⁺ (calculated)
	C ₆ H ₁₀ ON ₂ Na	149.0690	149.0691

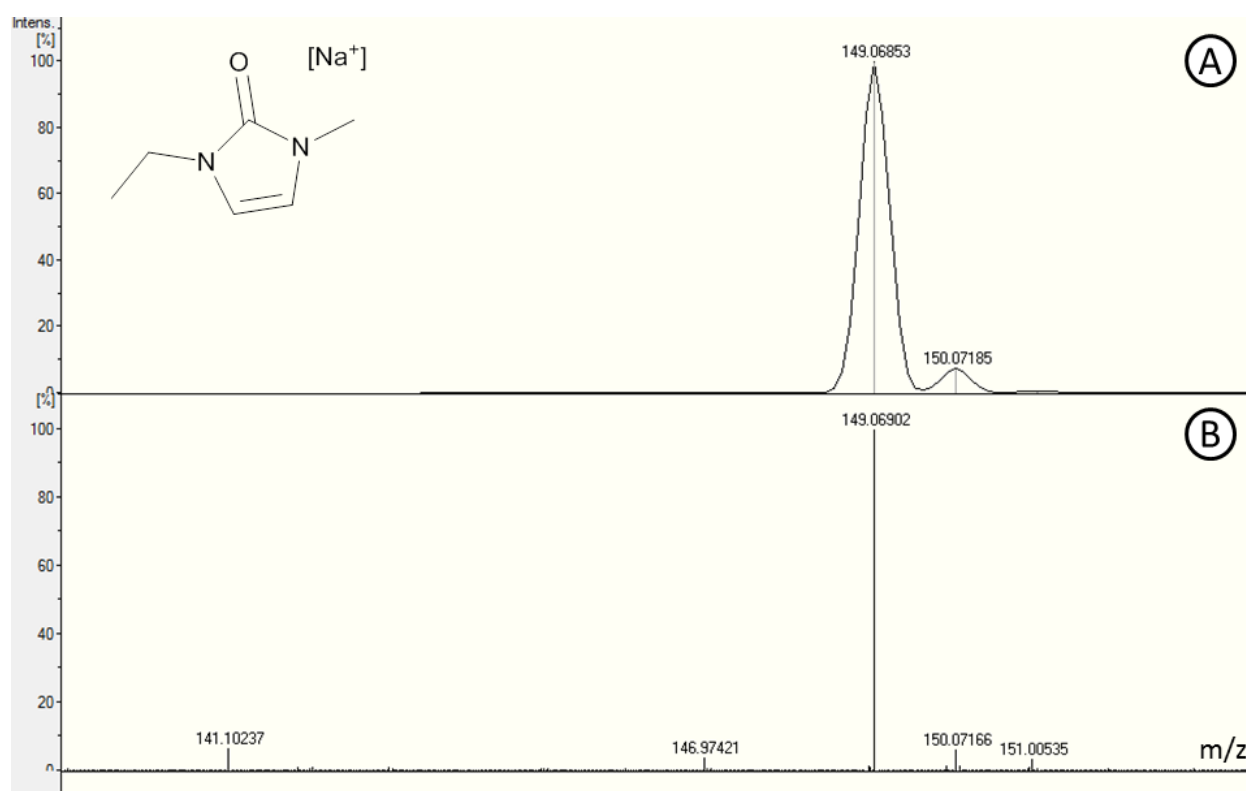


Figure S43. HRESI-MS spectra of molecular ion for the azolone C₆H₁₀ON₂Na. A. Calculated; B. Found

S8. Single crystal X-ray structure determination

Appropriate crystals of **19** and **20** were obtained from the reaction mixture in the IL according to the procedure reported in the related manuscript. Then, a suitable crystal was selected and placed on a diffractometer. The crystal was kept at 100(2) K during data collection. Using Olex2 [1], the structure was solved with the ShelXS [2] structure solution program using Direct Methods and refined with the ShelXL [3] refinement package using CGLS minimization.

1. O. V. Dolomanov, L. J. Bourhis, R. J. Gildea, J. A. K. Howard and H. Puschmann, OLEX2: a complete structure solution, refinement and analysis program. *J. Appl. Cryst.* (2009). 42, 339-341.
2. SHELXS, G.M. Sheldrick, *Acta Cryst.* (2008). A64, 112-122
3. SHELXL, G.M. Sheldrick, *Acta Cryst.* (2008). A64, 112-122

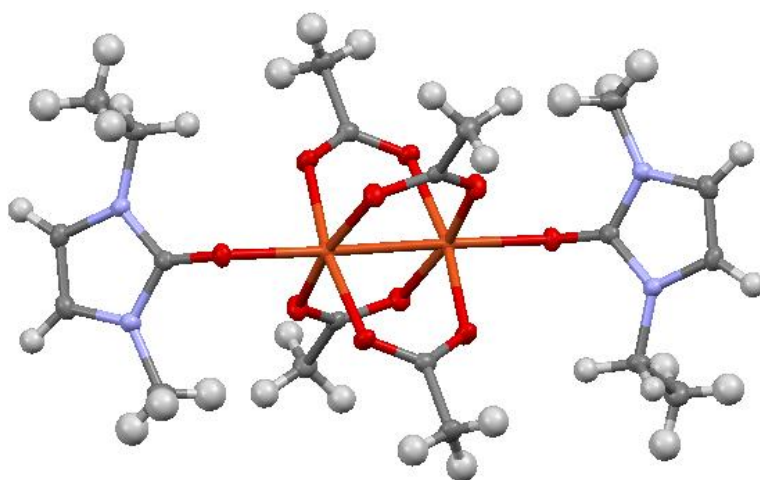


Figure S44. Crystal structure of the complex **19**¹.

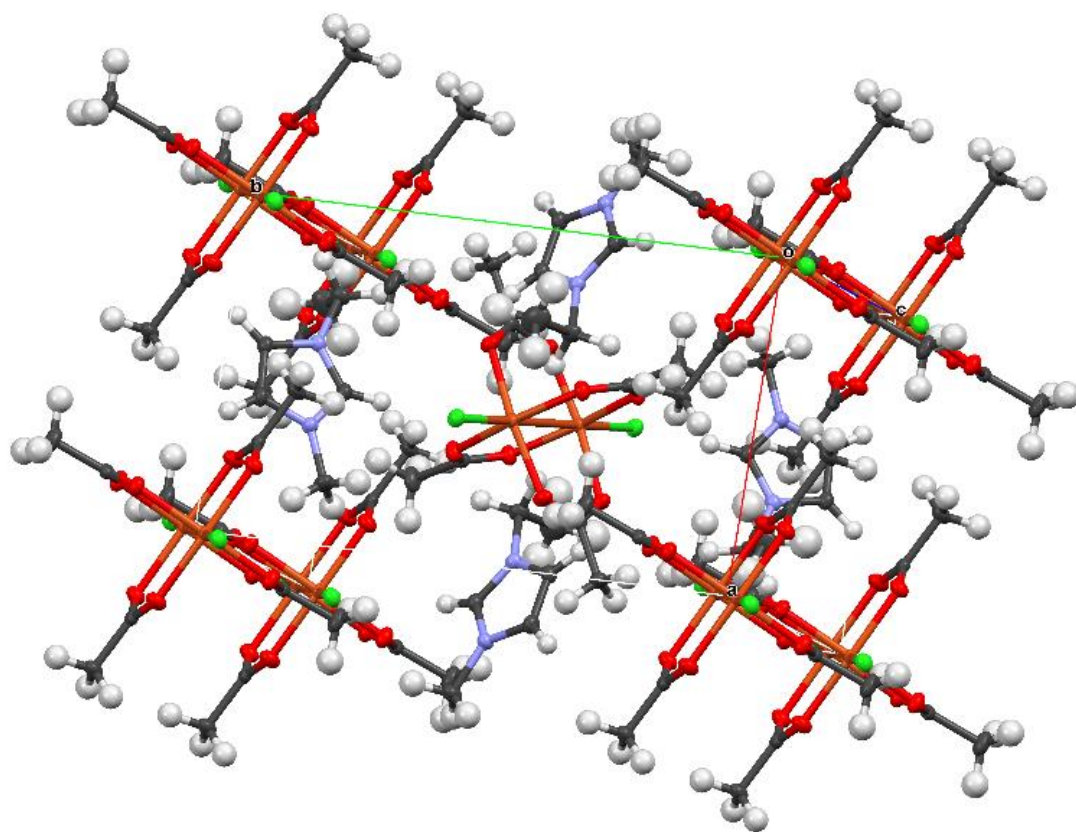


Figure S45. Crystal structure of the complex **20²**.

S9. Details on electrochemical experiments

For the electrochemical experiments ElectraSyn device was used (by IKA). All the electrodes are commercially available (working electrodes, reference electrode and counter electrodes).

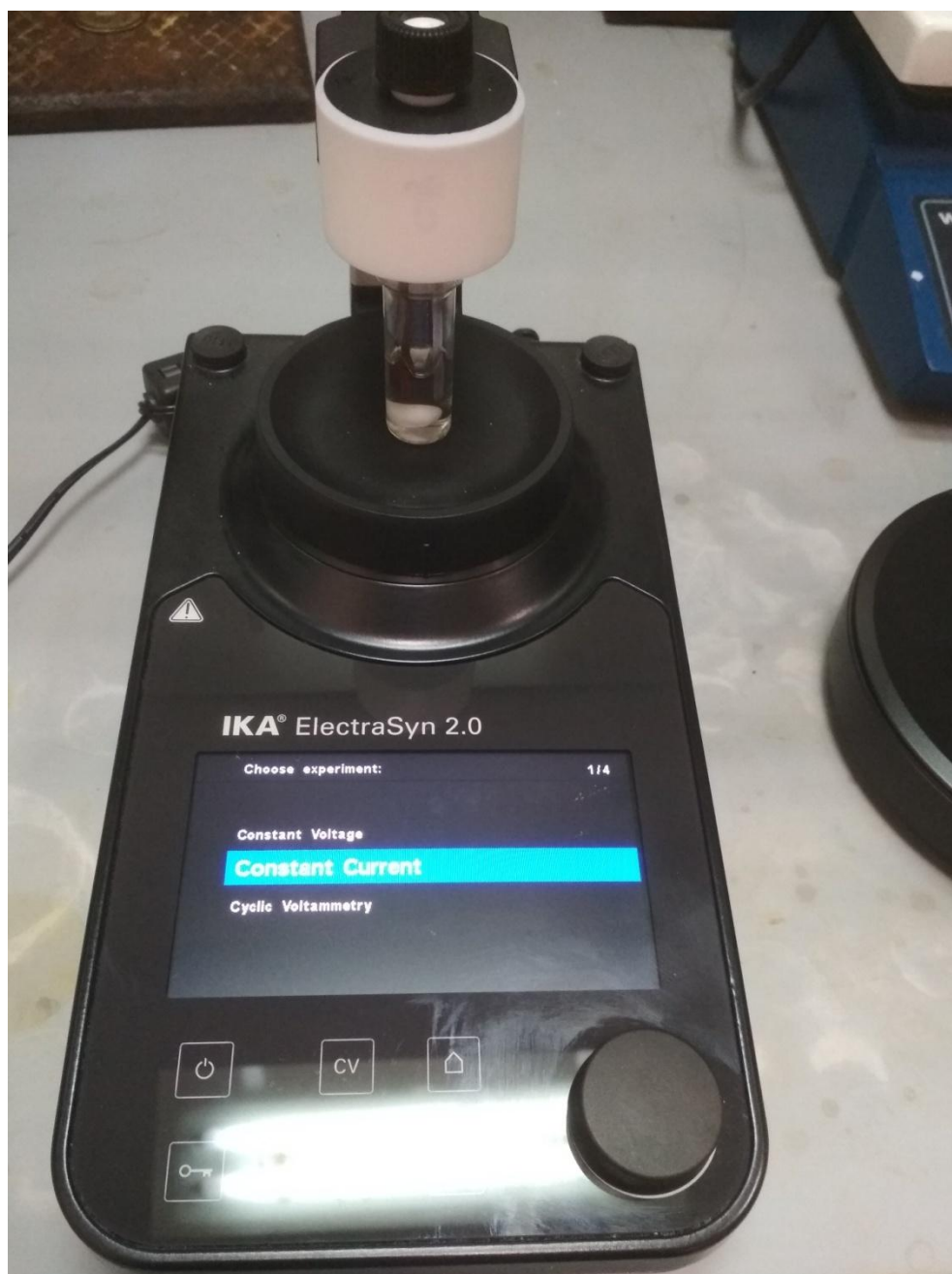


Figure S46. IKA ElectraSyn 2.0 device before experiments.



Figure S47. ElectraSyn device equipped with a single vial with two standard electrodes.



Figure S49. ElectraSyn apparatus equipped with a carousel.



Figure S50. ElectraSyn apparatus equipped with a carousel.

S10. References

1. V. G. Shtyrin, N. Y. Serov, D. R. Islamov, A. L. Konkin, M. S. Bukharov, O. I. Gnezdilov, D. B. Krivolapov, O. g. N. Kataeva, G. A. Nazmutdinova and F. Wendler, *Dalton Trans.*, 2014, **43**, 799-805.
2. N. Y. Serov, V. G. Shtyrin, D. R. Islamov, O. N. Kataeva and D. B. Krivolapov, *Acta Crystallographica Section E*, 2018, **74**, 981-986.